manufacturer's instructions. For cytokine profiling of a HTLV-1–specific $CD4^+$ T cell line, cells were stimulated with formaldehyde-fixed ILT-#350 for 48 h. Culture supernatant was collected, and various cytokines were measured using a Human Th1/Th2/Th17 Cytokine Kit for a Cytokine Beads Array (BD Biosciences).

Induction of HTLV-1–specific $CD4^+$ T cell line (T4 cells)

PBMCs (1×10^6 cells/ml) from patient #350, in complete remission at 180 d after allo-HSCT, were cultured for 2 wk with 100 nM Tax301–309 peptide in 96-well round-bottom tissue culture plate (BD Biosciences) in a final volume of 200 μl RPMI 1640 medium with 20% FCS and 10 U/ml rhIL-2. $CD4^+$ cells were then isolated by negative selection using a Human CD4 T lymphocyte Enrichment Set-DM (BD Biosciences) and maintained in RPMI 1640 medium with 20% FCS and 100 U/ml rhIL-2. Cells (1×10^6 cells/ml) were stimulated with formaldehyde-fixed ILT-#350 (2.5×10^5 cells/ml) every 2–3 wk. After multiple rounds of stimulation, the resulting $CD4^+$ T cell line was assessed for HTLV-1 specificity by comparing IFN-γ production against ILT-#350 to that against an HTLV-1–negative cell line, LCL-#350.

RT-PCR

Total RNA from cells was isolated using Isogen (Nippon Gene, Tokyo, Japan) and Turbo DNA-free (Life Technologies). First-strand cDNA was prepared from 0.5 μg RNA using ReverTra Ace and $Oligo(dT)_{20}$ primers provided in a ReverTra Ace-α-kit (Toyobo, Osaka, Japan). PCRs were performed in 50 μl reaction mixture containing ReverTra Dash (Toyobo), 0.5 μM of each HTLV-1 pX-specific primer (pX1, 5′-CCA CTT CCC AGG GTT TAG ACA GAT CTT C-3′ and pX4, 5′-TTC CTT ATC CCT CGA CTC CCC TCC TTC CCC-3′), and 2 μl cDNA. GAPDH-specific primers (GAPDH5′, 5′-ACC ACA GTC CAT GCC ATC AC-3′; GAPDH3′, 5′-TCC ACC ACC CTG TTG CTG TA-3′) were used as an internal control. The thermal cycling conditions comprised an initial activation step at 94°C for 1 min, followed by 30 cycles of denaturation (98°C, 10 s), annealing (60°C, 2 s), and extension (74°C, 30 s). The PCR amplicons were visualized by ethidium bromide staining following 2% (w/v) agarose gel electrophoresis.

Flow cytometry

For cell surface staining, the following fluorochrome-conjugated mouse anti-human mAbs were used: CD3-FITC (UCHT1; BioLegend, San Diego, CA), CD4-FITC (RPA-T4; BioLegend), CD8-FITC (RPA-T8; BioLegend), and CD8-PE-Cy5 (HIT8a; BD Biosciences, San Jose, CA). For tetramer staining, PE-conjugated HLA-A*0201/Tax11–19, HLA-A*1101/Tax88–96, HLA-A*1101/Tax272–280, and HLA-A*2402/Tax301–309 tetramers were purchased from Medical & Biological Laboratories (Nagoya, Japan). PE-conjugated HLA-DRB1*0101/Tax155–167 tetramer were newly generated through the custom service of Medical & Biological Laboratories. Whole-blood or cultured cells were stained with PE-conjugated Tax/HLA tetramer in conjunction with CD3-FITC and CD8-PE-Cy5 or CD4-PE-Cy5. For whole-blood samples, RBCs were lysed and fixed in BD FACS lysing solution (BD Biosciences) before washing. Samples were analyzed on a FACSCalibur (BD Biosciences), and data analyses were performed using FlowJo software (Tree Star, Ashland, OR).

Epitope mapping

T4 cells (3×10^5 cells/ml) were stimulated with LCL-#350, pulsed with various concentrations of synthetic peptides for 1 h at 37°C, at a responder/stimulator (R/S) ratio of 3. The culture supernatant was collected at 6 h poststimulation, and peptide-specific IFN-γ production from T4 cells was determined by ELISA.

HLA class II restriction assay

T4 cells (5×10^5 cells/ml) were cocultured for 6 h with ILT-#350 (1×10^5 cells/ml) in the presence or absence of anti-human HLA-DR (10 μg/ml; L243; BioLegend), anti-human HLA-DQ (10 μg/ml; SPVL3; Beckman Coulter, Fullerton, CA), or anti–HLA-ABC (10 μg/ml; W6/32; BioLegend). The IFN-γ in the supernatant was measured by ELISA.

To identify a HLA class II molecule responsible for Ag presentation to T4 cells, Tax155–167 peptide-specific IFN-γ responses were evaluated using various HLA-typed LCLs (LCL-#350, LCL-#341, LCL-#307, and LCL-Kan). These LCLs (1×10^5 cells/ml) were pulsed with 100 ng/ml Tax155–167 peptide for 1 h, fixed with 2% formaldehyde, and then cultured with T4 cells (3×10^5 cells/ml) for 6 h. The culture supernatant was collected, and IFN-γ in the supernatant was measured by ELISA.

Tetramer-based proliferation assay

PBMCs (1.0×10^6 cells/ml) were cultured for 13 or 14 d with or without 100 nM antigenic peptides in the presence of 10 U/ml rhIL-2. Cells were stained with HLA/Tax tetramer-PE, CD3-FITC, and CD8-PE-Cy5 or CD4-PE-Cy5 and then analyzed by flow cytometry.

Statistic analysis

Statistical significance was evaluated with the unpaired t test using Graphpad Prism 5 (Graphpad Software, La Jolla, CA). In all cases, two-tailed p values <0.05 were considered significant.

Results

Tax-specific T cell responses in ATL patients who received allo-HSCT with RIC

We previously reported that Tax-specific $CD8^+$ T cells were induced in some ATL patients after allo-HSCT with RIC from HLA-identical sibling donors (10). In this study, we examined the Tax-specific T cell response in a larger number of ATL patients who received allo-HSCT with RIC. Table I provides a summary of the

Table I. Clinical information and summary for Tax-specific $CD8^+$ T cells in 18 ATL patients at 180 d post–allo-HSCT with RIC

ID (Age, Sex)	ATL Subtype	Type of Donor	Donor-HLA	Donor HTLV-1 Sero Status	Chimerism (%)[a]	Tetramer (%)[b]	Proviral Load[c]
239 (55, M)	Lymphoma	r-PB	A 26/33, DR 4/13	(−)	<5	NT	0.1
241 (61, F)	Acute	r-PB	A 2/26, DR 10/18	(−)	<5	0.00	0.1
247 (52, F)	Lymphoma	r-PB	A 24/−, DR 9/15	(−)	<5	0.07	0.1
270 (57, M)	Lymphoma	r-PB	A 24/33, DR 13/15	(−)	<5	0.00	0.0
300 (53, F)	Lymphoma	r-PB	A 24/26, DR 4/15	(+)	<5	1.34	4.8
301 (57, F)	Acute	ur-BM	A 24/33, DR 13/15	(−)	<5	0.72	0.0
307 (68, F)	Acute	r-PB	A 2/11, DR 14/15	(+)	<5	0.10	5.4
317 (60, M)	Acute	ur-BM	A 2/24, DR 14/15	(−)	<5	0.92	0.0
328 (62, M)	Acute	ur-BM	A 11/24, DR 8/9	(−)	<5	0.75	NT
340 (50, M)	Acute	r-PB	A 2/24, DR 4/8	(−)	<5	1.40	0.7
341 (61, F)	Acute	ur-BM	A 24/33, DR 1/15	(−)	<5	0.45	0.1
344 (58, M)	Lymphoma	ur-BM	A 2/24, DR 4/−	(−)	<5	0.44	0.0
349 (53, M)	Acute	r-PB	A 24/−, DR 8/15	(+)	<5	0.00	0.0
350 (60, F)	Acute	ur-BM	A 24/26, DR 1/14	(−)	<5	0.59	0.6
351 (57, F)	Acute	ur-BM	A 24/26, DR 9/12	(−)	<5	0.45	0.0
358 (63, F)	Lymphoma	r-PB	A 2/11, DR 4/14	(−)	<5	0.42	0.0
352 (61, M)	Acute	ur-BM	A 11/26, DR 8/15	(−)	<5	0.14	0.0
364 (52, M)	Acute	r-PB	A 24/26, DR 1/−	(−)	<5	0.11	0.0

[a]Indicates percentage of recipient-derived T cell chimerism.
[b]Indicates percentage of tetramer$^+$ cells among $CD8^+$ T cells in PBMCs.
[c]Indicates copy number per 1000 PBMCs.
F, Female; M, male; NT, not tested; r-PB, related donor-derived peripheral blood stem cell; ur-BM, unrelated donor-derived bone marrow cell.

results of Tax-specific $CD8^+$ T cell detection by flow cytometry, using the Tax/HLA tetramers, in the peripheral blood of 18 ATL patients at 180 d after allo-HSCT, together with clinical information. During this period, all patients achieved a complete chimera state consisting of >95% of donor-derived hematopoietic cells. By using four available tetramers (HLA-A*0201/Tax11–19, HLA-A*2402/Tax301–309, HLA-A*1101/Tax88–96, and HLA-A*1101/Tax272–280), Tax-specific $CD8^+$ T cells were found in 14 patients. Because the donors were uninfected individuals in the majority of cases (Table I), induction of the Tax-specific donor-derived $CD8^+$ T cells in recipients indicated the presence of newly occurring immune responses against HTLV-1 in the recipients. This evidence strengthens our previous observation (10, 32).

We also used a GST–Tax fusion protein-based assay to evaluate Tax-specific T cell responses. The tetramer-based assay was limited to four kinds of epitopes and restricted by three HLA alleles but did not detect T cells directed to other epitopes or HLAs. The GST–Tax fusion protein-based assay can detect both $CD4^+$ and $CD8^+$ T cell responses, irrespective of HLA types. However, this sensitivity is not as good as single-cell analysis by flow cytometry (31). As shown in Fig. 1A, there was a wide variation in the IFN-γ responses to the Tax protein in the PBMCs among the 16 patients tested. In five patients (#247, #270, #328, #340, and #349), IFN-γ production of PBMCs against GST–TaxABC proteins was very low or not specific for the Tax protein. PBMCs from the other 11 patients (#239, #241, #301, #317, #341, #344, #350, #351, #352, #358, and #364) produced higher amounts of IFN-γ in response to GST–TaxABC proteins compared with GST. However, the levels of IFN-γ production varied among the patients.

We also evaluated the extent to which Tax-specific $CD4^+$ T cells were responsible for IFN-γ in the GST–Tax-based immunoassay system. We used PBMCs from patients #350 and #341, who showed high Tax-specific T cell responses. $CD8^+$ cell–depleted PBMCs from patient #350 and #341 showed a reduced but still significant level of Tax-specific IFN-γ–producing response compared with whole PBMCs (Fig. 1B). These results indicate that not only $CD8^+$ but also $CD4^+$ T cells against Tax are present in the peripheral blood from patient #350 and #341 after allo-HSCT with RIC.

Induction of an HTLV-1–specific $CD4^+$ T cell line from patient #350

We next attempted to induce HTLV-1–specific $CD4^+$ T cells from the PBMCs of patient #350 at 180 d after allo-HSCT, using an HTLV-1–infected T cell line (ILT-#350) as APCs. Freshly isolated PBMCs were stimulated for 2 wk with Tax301–309, a dominant CTL epitope presented by HLA-A*2402, to eliminate HTLV-1–infected cells, which potentially existed in PBMCs. The $CD4^+$ cells were then isolated from the cultured cells and stimulated with formaldehyde-fixed ILT-#350 every 2–3 wk. The established cell line was found to be a $CD4^+$ T cell line (designated as T4 cells thereafter) because cells expressed CD3 and CD4 but not CD8

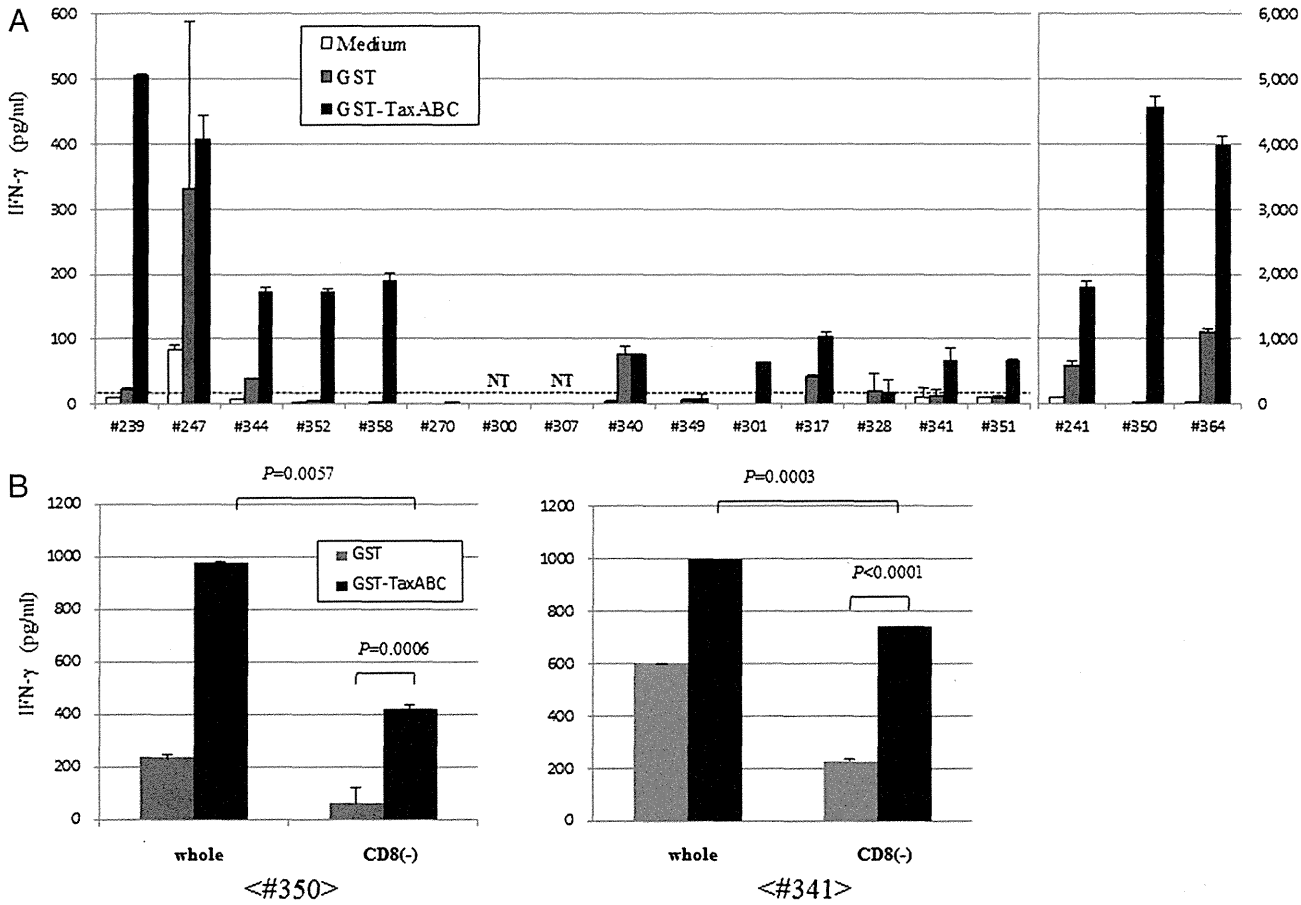

FIGURE 1. Diversity of Tax-specific T cell responses in ATL patients who received allo-HSCT with RIC. (**A** and **B**) PBMCs from 18 ATL patients at 180 d after allo-HSCT (A) or whole and $CD8^+$ cell–depleted PBMCs from two patients at 540 d after allo-HSCT (#350 and #341) (B) were cultured for 4 d in the absence (open square) or presence of GST (gray square), or GST–Tax (black square) proteins. The concentration of IFN-γ in the supernatant was determined by ELISA. The *y*-axis on the right side indicates the results from three patients (#241, #350, and #364). The dotted horizontal line indicates the detection limit (23.5 pg/ml). The error bars represent SD of duplicated wells. The representative result of two independent experiments is shown in (B).

(Fig. 2A). Because HTLV-1 has been shown to preferentially infect $CD4^+$ T cells in vivo and in vitro (24), we examined HTLV-1 expression in T4 cells by RT-PCR (Fig. 2B). As expected, the T4 cells did not express HTLV-1 Tax, indicating that the cells were not infected with HTLV-1. We assessed expression of various cytokines in T4 cells (Fig. 2C). The T4 cells were stimulated with formaldehyde-fixed ILT-#350 or LCL-#350. The cells produced large amounts of IFN-γ and TNF-α and small amounts of IL-2, IL-4, and IL-10 in response to ILT-#350 but not against LCL-#350. IL-6 and IL-17A were not detected in the culture supernatant. These data indicate that T4 cells are mainly HTLV-1–specific $CD4^+$ Th1-like cells but contain minor populations to produce Th2 cytokines.

Determination of the minimum epitope recognized by T4 cells

Freshly isolated PBMCs in the patient #350 produced IFN-γ in response to GST–Tax (Fig. 1A). We expected that the epitope recognized by the T4 cells should be present in the Tax protein. We therefore examined whether the T4 line responded to Tax using LCL-#350 pulsed with GST–Tax proteins as APCs. As shown in Fig. 3A, the T4 cells produced significantly higher amounts of IFN-γ in response to GST–TaxABC and GST–Tax-B (residues 113–237) (31) but not GST–Tax-A (residues 1–127) (31) and -C (residues 224–353 (31), when compared with the GST control protein, indicating that the T4 cells recognized the central region (residues 113–237) of the Tax Ag. We next synthesized eight overlapping 25-mer peptides spanning the central region of Tax (residues 103–246) and analyzed their abilities to stimulate T4 cells (Table II). The cell line produced high amounts of IFN-γ only when stimulated with Tax154–178 (Fig. 3B). We then prepared four overlapping 15-mer peptides, covering residues 154–178 of Tax, to examine the IFN-γ responses of the T4 cells (Table II). Both Tax151–165 and Tax156–170-stimulated cells to induce IFN-γ responses but not at a comparable level to Tax154–178 (Fig. 3C). These results suggest that the epitope recognized by T4 cells might be present in the N-terminal half of Tax154–178. We therefore stimulated the cells with Tax154–168, Tax155–169, or Tax156–170. The cells showed higher IFN-γ responses against Tax154–168 and Tax155–169 than Tax156–170, indicating that the minimum epitope might be within residues 155–168 of Tax (Fig. 3D). To identify the minimum epitope recognized by T4 cells, we next synthesized three overlapping peptides of 12- to 14-mer lengths beginning at residue 155 of Tax (Table II). Tax155–167 induced IFN-γ responses in cells at a similar level to Tax155–169 and Tax155–168, although Tax155–166 did not (Fig. 3E). Moreover, IFN-γ production of cells in response to various concentrations of Tax155–167 was comparable to that against Tax155–169 and Tax155–168 (Fig. 3F). These data clearly show that the minimum epitope recognized by the T4 cells is Tax155–167.

*HLA-DRB1*0101 restriction of Tax-specific T4 cells*

To analyze HLA class II molecules involved in the presentation of the minimum epitope, T4 cells were stimulated with ILT-#350 in the presence or absence of anti–HLA-DR, -DQ, and anti-HLA class I blocking Abs. As shown in Fig. 4A, the addition of an anti–HLA-DR blocking Ab abrogated IFN-γ responses of the T4 cells against ILT#-350, indicating that the epitope was HLA-DR restricted.

We further investigated the HLA-DR alleles responsible for the presentation of the minimum epitope by using four HLA-typed LCLs displaying different HLA-DRs. As shown in Fig. 4B, the T4 cells responded by producing IFN-γ when Tax155–167 was presented by autologous LCL-#350 (DR1/14) and allogeneic LCL-#341 (DR1/15). These results clearly indicate that this epitope is presented by HLA-DRB1*0101 on APCs. We searched for a known HLA-DRB1*0101 motif in the identified epitope Tax155–167 and found that this epitope contained the HLA-DRB1*0101 motif (Fig. 4C) (33).

Enhancement of Tax-specific $CD8^+$ T cell expansion by Tax155–167-specific $CD4^+$ T cell help

As T4 cells were established from PBMCs of an HTLV-1–infected patient #350, it is suggested that Tax155–167-specific $CD4^+$ T cells may be maintained in the $HLA\text{-}DRB1*0101^+$ patient #350.

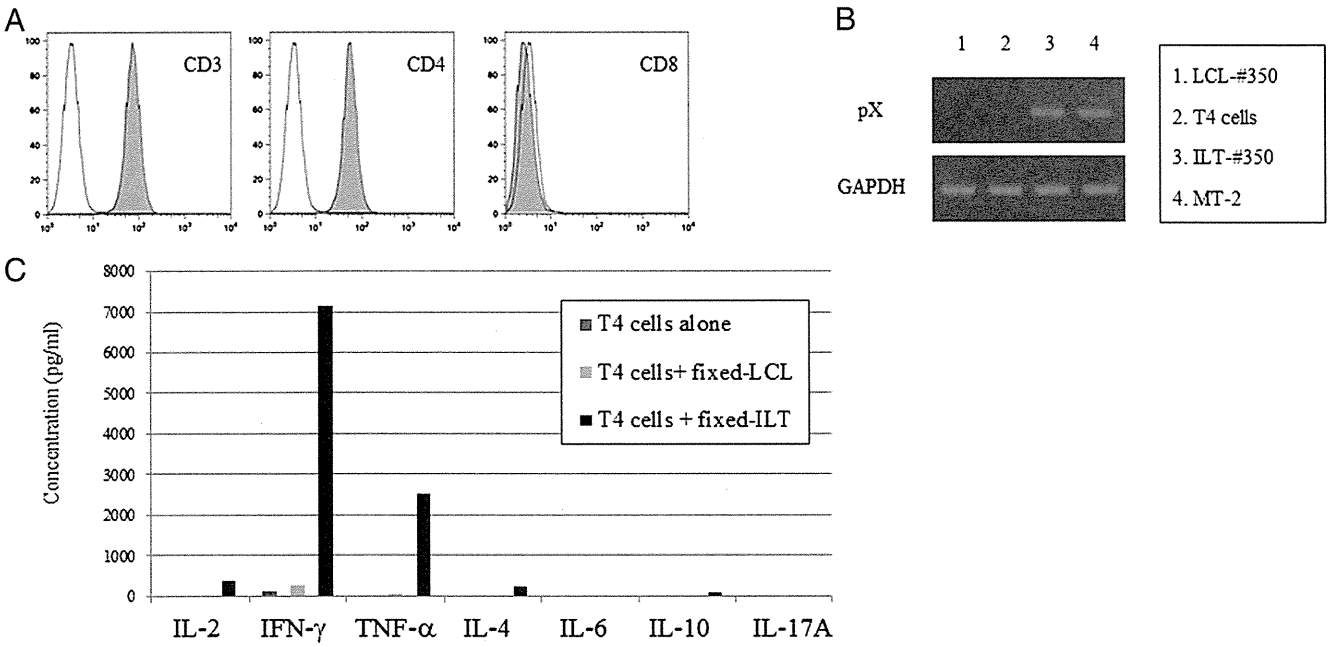

FIGURE 2. Phenotype and function of $CD4^+$ T cell line (T4) generated from patient #350. (**A**) Cell surface phenotype of T4 cells was analyzed by flow cytometry. (**B**) Total RNA was extracted from LCL-#350 (*lane 1*), T4 cells (*lane 2*), ILT-#350 (*lane 3*), and MT-2 (*lane 4*). Tax mRNA expression for each cell type was analyzed by RT-PCR. GAPDH was used as an internal control. (**C**) T4 cells were stimulated for 24 h with or without formaldehyde-fixed ILT-#350 or LCL-#350 cells. The concentration of indicated cytokines in the supernatants was measured using a cytometric bead array system.

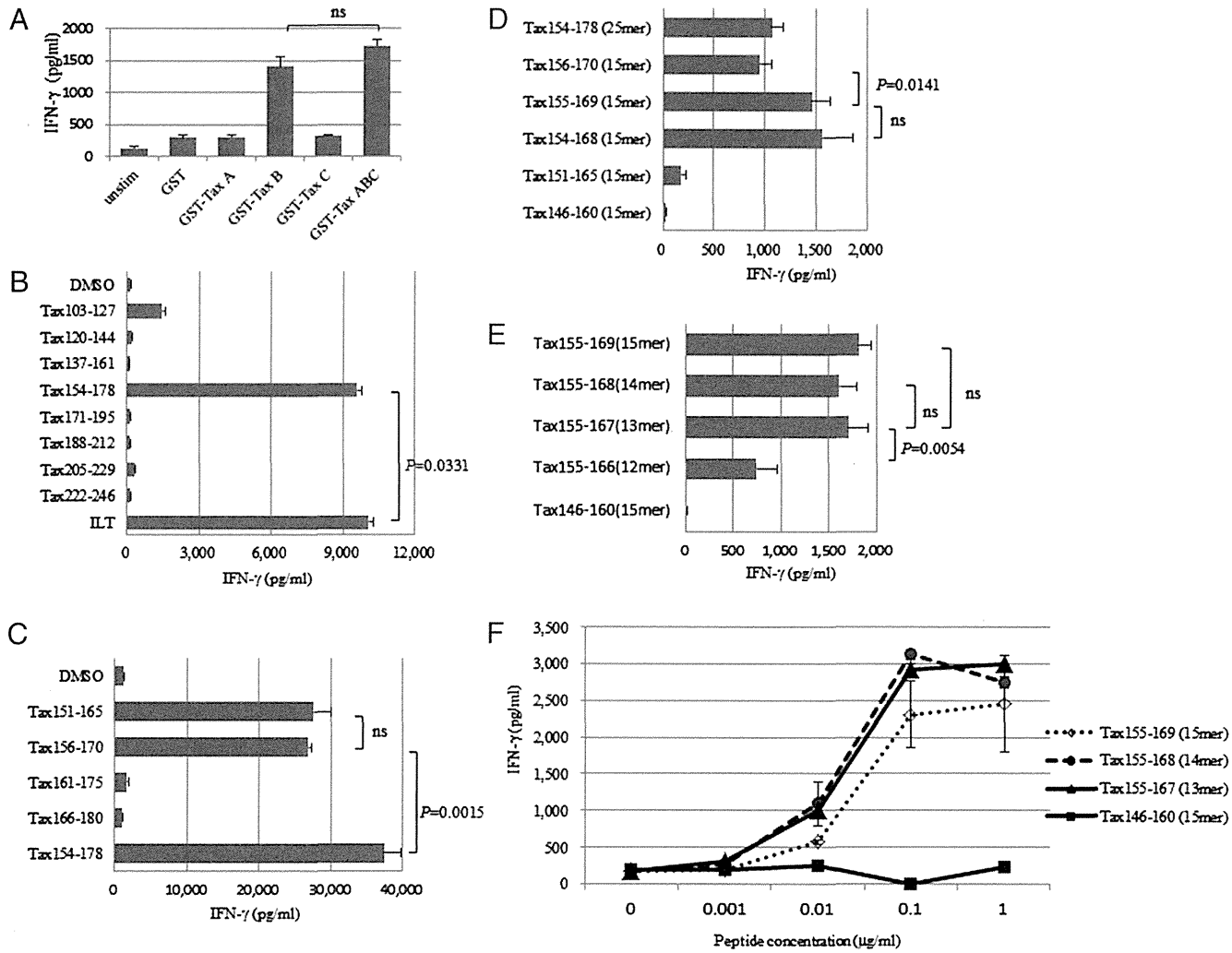

FIGURE 3. Identification of the dominant Tax-derived epitope recognized by established T4 cells. (**A**) Donor-derived LCL-#350 was pulsed with GST, GST–Tax-A, GST–Tax-B, GST–Tax-C, or a mixture of GST–Tax-A, -B, and -C (GST–TaxABC) for 24 h and then cocultured for 24 h with the T4 cells at a responder/stimulator (R/S) ratio of 3. IFN-γ production from T4 cells was analyzed by ELISA. (**B** and **C**) LCL-#350 was pulsed with the indicated overlapping 25-mer-long (B) or 15-mer-long (C) synthetic peptides (10 μg/ml) within the Tax-B region for 1 h. Formaldehyde-fixed ILT-#350 cells were cocultured with T4 cells for 6 h. IFN-γ in the supernatant was measured by ELISA. (**D** and **E**) IFN-γ responses of T4 cells were assessed using the indicated overlapping 12- to 25-mer-long synthetic peptides (100 ng/ml). (**F**) IFN-γ responses of T4 cells against indicated concentrations of 13- to 15-mer-long peptides were assessed as in (B) and (C). (A–F) Results are representative of two or three independent experiments. The error bars represent SD of triplicate wells. Statistical significance was analyzed by the unpaired *t* test.

We therefore evaluated the helper function of Tax155–167-specific $CD4^+$ T cells on the expansion of dominant Tax-specific CTLs in fresh PBMCs of the patient #350. Freshly isolated PBMCs from patient #350 (A24/26, DR1/14) at 540 d after allo-HSCT were stimulated for 13 d with the HLA-A24–restricted CTL epitope peptide (Tax301–309) in the presence or absence of the HLA-DRB1*0101–restricted $CD4^+$ Th epitope peptide (Tax155–167), and Tax-specific $CD8^+$ T cell expansion was evaluated using the HLA-A*2402/Tax301–309 tetramer. As shown in Fig. 5, Tax301–309-specific $CD8^+$ T cells proliferated to 9.26% of $CD8^+$ T cells when stimulated with Tax301–309 alone. Surprisingly, a highly elevated frequency (62.3%) of tetramer-binding $CD8^+$ T cells was detected by in vitro costimulation with Tax301–309 and Tax155–167, suggesting the presence of Tax155–167-specific $CD4^+$ Th cells in patient #350.

We examined whether Tax155–167-specific $CD4^+$ T cells existed and functioned as helper cells in the other two HTLV-1–infected HLA-DRB1*0101^+ patients after allo-HSCT (day 360 for patient #341 and day180 for #364). These patients had detectable levels of HLA-A*2402/Tax301–309 tetramer-binding $CD8^+$ T cells in the peripheral blood (Fig. 5). In patients #341 and #364, the tetramer-binding cells expanded to 7.7 and 0.849% of $CD8^+$ T cells at 13 d of culture when stimulated with the CTL epitope peptide, Tax301–309, alone. Costimulation of PBMCs with both peptides Tax155–167 and Tax301–309 led to a vigorous proliferation of tetramer-binding $CD8^+$ T cells (59.6% for patient #341 and 15.5% for patient #364) as observed in patient #350 (Fig. 5). These results indicate that Tax155–167-specific $CD4^+$ T cells may be present and contribute to enhancing $CD8^+$ T cell responses in HTLV-1–infected HLA-DRB1*0101^+ individuals after allo-HSCT.

*Tax155–167-specific $CD4^+$ T cells were maintained in HTLV-1–infected HLA-DRB1*0101^+ individuals*

We next generated the HLA-DRB1*0101/Tax155–167 tetramer to directly detect Tax155–167-specific $CD4^+$ T cells and examined the presence of Tax155–167-specific $CD4^+$ T cells in the PBMCs freshly isolated from two HLA-DRB1*0101^+ patients after allo-HSCT (day 180 for patient #350 and day 360 for patient #364).

Table II. Synthetic oligopeptides used in this study

Peptide	Sequence
Tax103–127	P S F L Q A M R K Y S P F R N G Y M E P T L G Q H
Tax120–144	M E P T L G Q H L P T L S F P D P G L R P Q N L Y
Tax137–161	G L R P Q N L Y T L W G G S V V C M Y L Y Q L S P
Tax154–178	M Y L Y Q L S P P I T W P L L P H V I F C H P G Q
Tax171–195	V I F C H P G Q L G A F L T N V P Y K R I E E L L
Tax188–212	Y K R I E E L L Y K I S L T T G A L I I L P E D C
Tax205–229	L I I L P E D C L P T T L F Q P A R A P V T L T A
Tax222–246	R A P V T L T A W Q N G L L P F H S T L T T P G I
Tax146–160	L W G G S V V C M Y L Y Q L S
Tax151–165	V V C M Y L Y Q L S P P I T W
Tax154–168	M Y L Y Q L S P P I T W P L L
Tax155–169	Y L Y Q L S P P I T W P L L P
Tax156–170	L Y Q L S P P I T W P L L P H
Tax161–175	P P I T W P L L P H V I F C H
Tax166–180	P L L P H V I F C H P G Q L G
Tax155–168	Y L Y Q L S P P I T W P L L
Tax155–167	Y L Y Q L S P P I T W P L
Tax155–166	Y L Y Q L S P P I T W P

Tax155–167-specific CD4$^+$ T cells were detected ex vivo in the patient #350 (0.11%) and proliferated to 11.6% among CD4$^+$ T cells at 13 d poststimulation with Tax155–167 peptide. In the patient #364, tetramer-binding CD4$^+$ T cells were undetectable in fresh PBMCs but expanded to 0.37% by in vitro stimulation with Tax155–167 peptide (Fig. 6A). In an HLA-DRB1*0101$^+$–seronegative donor #365, Tax155–167-specific CD4$^+$ T cells were not found in fresh PBMCs and did not become detectable at 13 d after stimulation with Tax155–167 peptide (Fig. 6A). This result indicates that Tax155–167-specific CD4$^+$ T cells are maintained and possesses the abilities to proliferate in response to HTLV-1 Tax in these patients.

We further examined whether Tax155–167-specific CD4$^+$ T cells existed in two HTLV-1–infected individuals carrying HLA-DRB1*0101, an AC #310 and a HAM/TSP patient #294, and detected 0.18 and 0.31% of tetramer-binding cells in peripheral CD4$^+$ T cells, respectively (Fig. 6B). These results suggest that Tax155–167-specific CD4$^+$ T cells are maintained in HTLV-1–infected individuals expressing an HLA-DRB1*0101 allele, regardless of HSCT.

Discussion

In this study, we demonstrated Tax-specific CD4$^+$ T cell responses in some ATL patients post–allo-HSCT and identified a novel HLA-DRB1*0101–restricted CD4 T cell epitope, Tax155–167, which was recognized by HTLV-1–specific CD4$^+$ T cells and consequently led to robust Tax-specific CD8$^+$ T cell expansion. We also found that Tax155–167-specific CD4$^+$ T cells existed in all HTLV-1–infected HLA-DRB1*0101$^+$ individuals tested, regardless of HSCT, by newly generated HLA-DRB1*0101/Tax155–167 tetramers. These results suggest that Tax155–167 might be a dominant epitope recognized by HTLV-1–specific CD4$^+$ T cells

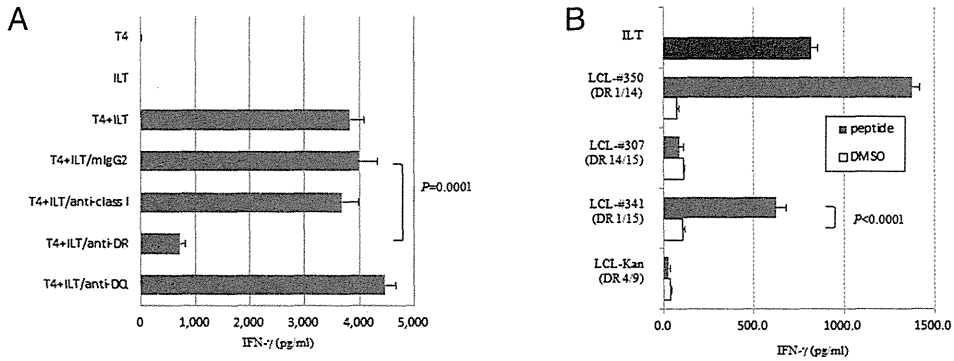

C

	Relative position												
	1	2	3	4	5	6	7	8	9	10	11	12	13
Tax155-167	**Y**	**L**	**Y**	**Q**	**L**	**S**	**P**	**P**	**I**	**T**	**W**	**P**	**L**
Anchor residues	Y,V, L,F, I,A M,W	*	*	L,A, I,V, M,N, Q	*	A,G, S,T, P	*	*	L,A, I,V, N,F, Y				

FIGURE 4. HLA-DRB1*0101 restriction of Tax155–167 recognition by established T4 cells. (**A**) T4 cells were cocultured for 6 h with ILT-#350 in the presence or absence of the following blocking Abs (10 μg/ml): anti-human HLA-DR; anti-human HLA-DQ; anti–HLA-class I; or isotype control. IFN-γ production from T4 cells was measured by ELISA. (**B**) The T4 cells were cocultured for 6 h with autologous (#350) or allogeneic (#307, #341, and Kan) LCLs pulsed with (closed bar) or without (open bar) Tax155–167 for 1 h or with recipient-derived ILT-#350. The HLA-DR alleles of each LCL line are indicated in parentheses. IFN-γ production of T4 cells was assessed by ELISA. (A and B) Representative data of three independent experiments are shown. The error bars represent SD of triplicate wells. Statistical significance was analyzed by the unpaired *t* test. (**C**) The amino acid sequence between residues 155 and 167 of Tax contained a putative HLA-DRB1*0101 anchor motif (33).

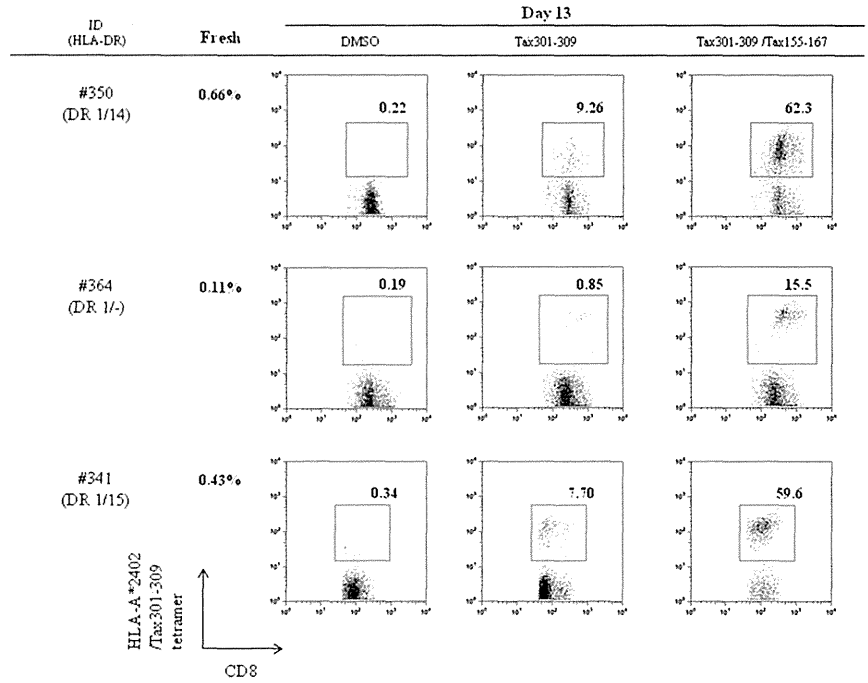

FIGURE 5. Augmentation of Tax-specific $CD8^+$ T cell expansion by costimulation with CTL epitope and Tax155–167 peptides. PBMCs from HLA-DRB1*0101– and HLA-A24–expressing ATL patients (#350, #364, and #341) who underwent allo-HSCT with RIC were cultured for 13 d in the presence of DMSO, 100 nM CTL epitope (Tax301–309), or a mixture of Tax301–309 (100 nM) and Tax155–167 (100 nM) peptides. Data indicate percentages of HLA-A*2402/Tax301–309 $tetramer^+$ cells among $CD3^+CD8^+$ T cells. Fresh indicates frequency of HLA-A*2402/Tax301–309 $tetramer^+CD8^+$ T cells detected in fresh peripheral blood.

in HTLV-1–infected individuals expressing HLA-DRB1*0101 and that Tax-specific $CD4^+$ T cells might efficiently induce HTLV-1–specific CTL expansion to strengthen the graft-versus-ATL effects in ATL patients after allo-HSCT.

In HTLV-1 infection, analysis of virus-specific $CD4^+$ T cell responses appears to be limited because $CD4^+$ T cells are preferentially infected with HTLV-1 (24, 34, 35), and HTLV-1 Ags are produced from infected cells at a few hours postculture (34, 36). In this study, we used blood samples from 18 ATL patients after allo-HSCT with RIC and from HLA identical–related or unrelated donors and found that these recipients had undetectable or very low proviral loads (Table I), as previously shown (7–9). We previously reported that Tax-specific CTLs were induced in some patients with complete remission after allo-HSCT for ATL and might contribute to the graft-versus-leukemia effect (10). In the current study, Tax-specific T cell responses or tetramer-binding $CD8^+$ T cells were detected in 68.8% (11 of 16) or 82.4% (14 of 17) of patients tested, respectively (Fig. 1A, Table I). In addition, helper function of Tax-specific $CD4^+$ T cells to enhance Tax-specific $CD8^+$ T cell expansion was observed in PBMCs from all three HLA-DRB1*0101^+ patients tested (Fig. 5). These data suggest that both $CD8^+$ and $CD4^+$ Tax-specific T cell responses might contribute to elimination of remaining leukemic and/or infected cells in some patients having T cell responses against Tax. However, given the fact that not all ATL patients who achieved complete remission after allo-HSCT had Tax-specific $CD8^+$ T cells, graft-versus-host reaction may mainly contribute to achieve complete remission after allo-HSCT. It is of note that Tax-specific

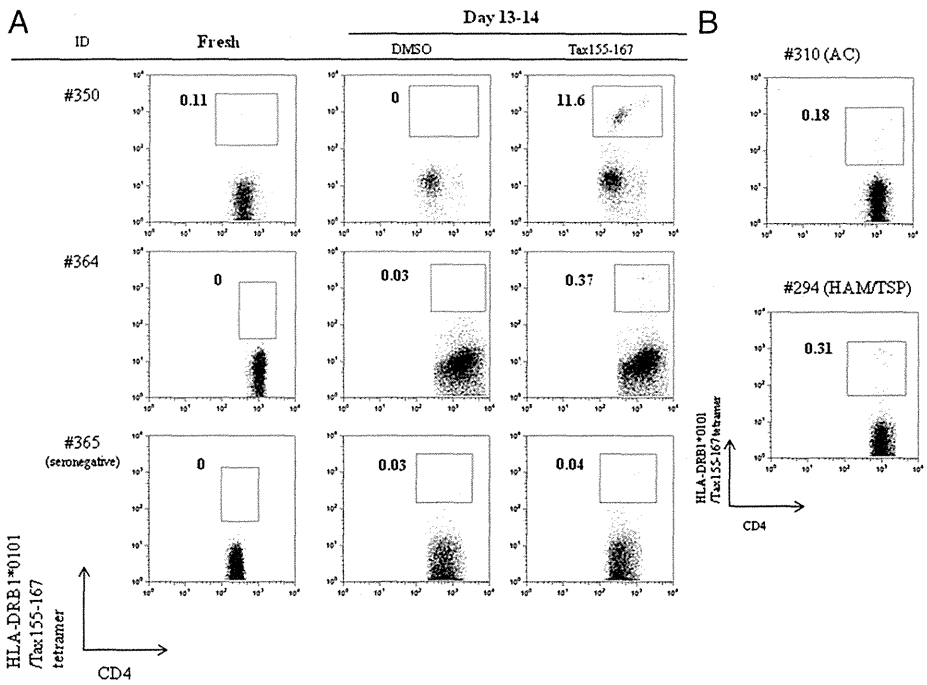

FIGURE 6. Detection of Tax155–167-specific $CD4^+$ T cells in HTLV-1–infected HLA-DRB1*0101^+ individuals. (**A**) In two ATL patients after allo-HSCT (#350 and #364) and an HLA-DRB1*0101^+–seronegative donor (#365), frequency of HLA-DRB1*0101/Tax155–167 tetramer-binding $CD4^+$ T cells was analyzed in fresh PBMCs and PBMCs cultured for 13–14 d in the presence of Tax155–167 (100 nM) peptide. Data indicate percentages of $tetramer^+$ cells in $CD3^+CD4^+$ T cells. (**B**) Frequency of HLA-DRB1*0101/Tax155–167 tetramer-binding $CD4^+$ T cells in fresh PBMCs from an AC #310 and an HAM/TSP patient #294 was analyzed. Data indicate percentages of $tetramer^+$ cells in $CD3^+CD4^+$ T cells.

T cell responses were detected in 57.1% (four of seven) or 87.5% (seven of eight) of the patients after allo-HSCT with RIC from HTLV-1–seronegative sibling or unrelated donors, respectively. A Tax-specific T cell response was not detected in three patients who underwent allo-HSCT from seropositive donors (Fig. 1, Table I).

It has been proposed that CTLs are the main effector cells against many pathogenic viruses, including HTLV-1. To date, many CTL epitopes recognized by HTLV-1–specific CTLs have been identified, some of which are thought to be the candidates of peptide-based T cell immunotherapy (10, 20, 32, 37–40). $CD4^+$ T cells have also been known to be critical for induction and maintenance of Ag-specific $CD8^+$ T cells (15–19). With respect to HTLV-1 infection, there are several reports identifying HLA-DRB1*0101–restricted epitopes recognized by $CD4^+$ T cells against Env or Tax (Env380–394 (21), Env436–450, Env451–465, Env456–470 (23), and Tax191–205 (22)), which were established by stimulating PBMCs from uninfected or infected individuals with synthetic peptides. In this study, for determination of an epitope recognized by HTLV-1–specific $CD4^+$ T cells, we established an HTLV-1–specific $CD4^+$ T cell line from the patient #350 at 180 d after allo-HSCT by several stimulations with an HTLV-1 Ags-expressing T cell line (ILT-#350) from the same patient. In addition, we found that Tax155–167-specific $CD4^+$ T cells were present in peripheral blood from patient #350 at 180 and 540 d after all-HSCT, indicating that the epitope, Tax155–167, identified in this study is naturally presented on HTLV-1–infected cells and predominantly recognized by HTLV-1–specific $CD4^+$ Th cells in the patient #350 at least within 540 d after allo-HSCT. Another HLA-DRB1*0101–restricted Tax epitope, Tax191–205, has been reported previously (22). In this study, the amino acid sequence within this region was revealed to be conserved in the infected T cell line, ILT-#350 established from the patient #350 (data not shown), indicating that Tax191–205 can be presented on APCs and Tax191–205-specific $CD4^+$ T cells may be induced in patient #350. However, Tax155–167-specific but not Tax191–205-specific $CD4^+$ T cells were revealed to predominantly appear in the HTLV-1–specific T4 cell line, established from PBMCs in the patient #350 at 180 d after allo-HSCT. This suggests that in the case of patient #350 at 180 d after allo-HSCT, Tax191–205-specific $CD4^+$ T cells may not be the most frequent population among HTLV-1–specific $CD4^+$ T cells.

It has been known that Ag-specific effector and memory $CD4^+$ T cells are typically present at much lower frequencies than their $CD8^+$ counterparts and that MHC class II tetramer might have a weak TCR–MHC affinity (41). Although this limited affinity of MHC class II tetramer might preclude detection of Ag-specific low-affinity $CD4^+$ T cells, the low-affinity $CD4^+$ T cells, below detection with MHC class II tetramers, were also proved to be critical effectors in Ag-specific responses (42). In the current study, MHC class II tetramer analysis revealed that Tax155–167-specific $CD4^+$ T cells were present in HLA-DRB1*0101$^+$ HTLV-1–infected individuals: two ATL patients after allo-HSCT (day 180 for #350 and day 360 for #364), an AC #310, and a HAM/TSP patient #294 (Fig. 6). Because of a shortage of blood sample from patient #341, we could not perform the direct detection for Tax155–167-specific $CD4^+$ T cells by the MHC class II tetramers. However, enhanced expansion of Tax301–309-specific $CD8^+$ T cells was observed in patient #341 at 360 d after allo-HSCT when PBMCs were stimulated with Tax301–309 in the presence of Tax155–167 (Fig. 5). So far, Tax155–167-specific $CD4^+$ T cells were detected in fresh and/or Tax155–167-stimulated PBMCs of all HTLV-1–infected HLA-DRB1*0101$^+$ individuals tested, although their frequencies were various. These results suggest that Tax155–167 may be the dominant epitope recognized by Tax-specific $CD4^+$ T cells in HTLV-1–infected HLA-DRB1*0101$^+$ individuals. In ATL patients after HSCT, the donor-derived T cells reconstituted in recipients will first encounter HTLV-1 Ags, because HTLV-1 still persists in the patients even though proviral loads become undetectable in the peripheral bloods. Indeed, we found that donor-derived Tax155–167-specific $CD4^+$ T cells were present in three ATL patients after allo-HSCT from seronegative donors. This finding also suggests that Tax155–167-specific naive $CD4^+$ T cells may pre-exist in HLA-DRB1*0101$^+$ individuals and can be primed with HTLV-1 Ags during the primary infection. In this study, Tax155–167-specific $CD4^+$ T cells were also detected in an AC and a HAM/TSP patient (Fig. 6B), suggesting that Tax155–167-specific $CD4^+$ T cells may be maintained in some HLA-DR1$^+$ individuals during the chronic phase of HTLV-1 infection. However, it has been reported that epitope hierarchies may change because of T cell escape mutants (43, 44) and unresponsiveness or deletion of epitope-specific T cells because of prolonged Ag stimulation during chronic infection (45, 46). Further longitudinal studies with a number of samples will be required to confirm that Tax155–167 is a dominant epitope of HTLV-1–specific $CD4^+$ T cells in HLA-DRB1*0101$^+$–infected individuals in the course of HTLV-1 infection.

Among three patients (#241, #350, and #364) showing high T cell responses against recombinant Tax protein, two patients (#350 and #364) were found to carry HLA-DRB1*0101 and have efficient $CD4^+$ Th cell responses against Tax155–167. Intriguingly, it has been reported that HLA-DRB1*0101 is associated with susceptibility to HAM/TSP (47, 48). In addition, $CD4^+$ T cells have been shown to be the dominant cells infiltrating in early active inflammatory spinal cord lesions (28, 29) with spontaneous production of proinflammatory cytokines (30). These observations suggest that HLA-DRB1*0101 might be associated with susceptibility to HAM/TSP via an effect on high $CD4^+$ T cell activation. Further studies are needed to clarify whether HLA-DRB1*0101 is associated with high Tax-specific $CD4^+$ T cell responses in HTLV-1–infected individuals.

Early studies using lymphocytic choriomeningitis virus showed that $CD4^+$ T cell help is critical for maintenance of $CD8^+$ T cell function during chronic infections (18). It has also been suggested that $CD4^+$ T cells are required for optimal CTL responses during HTLV-1 infection (49). Aubert et al. (50) showed that both Ag-specific naive and effector $CD4^+$ T cell help rescued exhausted $CD8^+$ T cells in vivo, resulting in a decrease in viral burden. In the current study, we determined a novel HLA-DRB1*0101–restricted Th epitope, Tax155–167, which was capable of augmenting Tax-specific $CD8^+$ T cell expansion by stimulating Tax155–167-specific $CD4^+$ T cells. This epitope would be a useful tool for investigating the roles of HTLV-1–specific $CD4^+$ T cells in antitumor immunity and in pathogenesis of HTLV-1–related inflammatory diseases such as HAM/TSP and developing novel vaccines to prevent progression or recurrence of ATL.

Disclosures

The authors have no financial conflicts of interest.

References

1. Hinuma, Y., K. Nagata, M. Hanaoka, M. Nakai, T. Matsumoto, K. I. Kinoshita, S. Shirakawa, and I. Miyoshi. 1981. Adult T-cell leukemia: antigen in an ATL cell line and detection of antibodies to the antigen in human sera. *Proc. Natl. Acad. Sci. USA* 78: 6476–6480.
2. Poiesz, B. J., F. W. Ruscetti, A. F. Gazdar, P. A. Bunn, J. D. Minna, and R. C. Gallo. 1980. Detection and isolation of type C retrovirus particles from fresh and cultured lymphocytes of a patient with cutaneous T-cell lymphoma. *Proc. Natl. Acad. Sci. USA* 77: 7415–7419.

3. de Thé, G., and R. Bomford. 1993. An HTLV-I vaccine: why, how, for whom? *AIDS Res. Hum. Retroviruses* 9: 381–386.
4. Uchiyama, T. 1997. Human T cell leukemia virus type I (HTLV-I) and human diseases. *Annu. Rev. Immunol.* 15: 15–37.
5. Tsukasaki, K., T. Maeda, K. Arimura, J. Taguchi, T. Fukushima, Y. Miyazaki, Y. Moriuchi, K. Kuriyama, Y. Yamada, and M. Tomonaga. 1999. Poor outcome of autologous stem cell transplantation for adult T cell leukemia/lymphoma: a case report and review of the literature. *Bone Marrow Transplant.* 23: 87–89.
6. Utsunomiya, A., Y. Miyazaki, Y. Takatsuka, S. Hanada, K. Uozumi, S. Yashiki, M. Tara, F. Kawano, Y. Saburi, H. Kikuchi, et al. 2001. Improved outcome of adult T cell leukemia/lymphoma with allogeneic hematopoietic stem cell transplantation. *Bone Marrow Transplant.* 27: 15–20.
7. Tanosaki, R., N. Uike, A. Utsunomiya, Y. Saburi, M. Masuda, M. Tomonaga, T. Eto, M. Hidaka, M. Harada, I. Choi, et al. 2008. Allogeneic hematopoietic stem cell transplantation using reduced-intensity conditioning for adult T cell leukemia/lymphoma: impact of antithymocyte globulin on clinical outcome. *Biol. Blood Marrow Transplant.* 14: 702–708.
8. Choi, I., R. Tanosaki, N. Uike, A. Utsunomiya, M. Tomonaga, M. Harada, T. Yamanaka, M. Kannagi, and J. Okamura. 2011. Long-term outcomes after hematopoietic SCT for adult T-cell leukemia/lymphoma: results of prospective trials. *Bone Marrow Transplant.* 46: 116–118.
9. Okamura, J., A. Utsunomiya, R. Tanosaki, N. Uike, S. Sonoda, M. Kannagi, M. Tomonaga, M. Harada, N. Kimura, M. Masuda, et al. 2005. Allogeneic stem-cell transplantation with reduced conditioning intensity as a novel immunotherapy and antiviral therapy for adult T-cell leukemia/lymphoma. *Blood* 105: 4143–4145.
10. Harashima, N., K. Kurihara, A. Utsunomiya, R. Tanosaki, S. Hanabuchi, M. Masuda, T. Ohashi, F. Fukui, A. Hasegawa, T. Masuda, et al. 2004. Graft-versus-Tax response in adult T-cell leukemia patients after hematopoietic stem cell transplantation. *Cancer Res.* 64: 391–399.
11. Jacobson, S., H. Shida, D. E. McFarlin, A. S. Fauci, and S. Koenig. 1990. Circulating $CD8^+$ cytotoxic T lymphocytes specific for HTLV-I pX in patients with HTLV-I associated neurological disease. *Nature* 348: 245–248.
12. Kannagi, M., S. Harada, I. Maruyama, H. Inoko, H. Igarashi, G. Kuwashima, S. Sato, M. Morita, M. Kidokoro, M. Sugimoto, et al. 1991. Predominant recognition of human T cell leukemia virus type I (HTLV-I) pX gene products by human $CD8^+$ cytotoxic T cells directed against HTLV-I-infected cells. *Int. Immunol.* 3: 761–767.
13. Shimizu, Y., A. Takamori, A. Utsunomiya, M. Kurimura, Y. Yamano, M. Hishizawa, A. Hasegawa, F. Kondo, K. Kurihara, N. Harashima, et al. 2009. Impaired Tax-specific T-cell responses with insufficient control of HTLV-1 in a subgroup of individuals at asymptomatic and smoldering stages. *Cancer Sci.* 100: 481–489.
14. Takamori, A., A. Hasegawa, A. Utsunomiya, Y. Maeda, Y. Yamano, M. Masuda, Y. Shimizu, Y. Tamai, A. Sasada, N. Zeng, et al. 2011. Functional impairment of Tax-specific but not cytomegalovirus-specific $CD8^+$ T lymphocytes in a minor population of asymptomatic human T-cell leukemia virus type 1-carriers. *Retrovirology* 8: 100.
15. Cardin, R. D., J. W. Brooks, S. R. Sarawar, and P. C. Doherty. 1996. Progressive loss of $CD8^+$ T cell-mediated control of a gamma-herpesvirus in the absence of $CD4^+$ T cells. *J. Exp. Med.* 184: 863–871.
16. Grakoui, A., N. H. Shoukry, D. J. Woollard, J. H. Han, H. L. Hanson, J. Ghrayeb, K. K. Murthy, C. M. Rice, and C. M. Walker. 2003. HCV persistence and immune evasion in the absence of memory T cell help. *Science* 302: 659-662.
17. Kalams, S. A., S. P. Buchbinder, E. S. Rosenberg, J. M. Billingsley, D. S. Colbert, N. G. Jones, A. K. Shea, A. K. Trocha, and B. D. Walker. 1999. Association between virus-specific cytotoxic T-lymphocyte and helper responses in human immunodeficiency virus type 1 infection. *J. Virol.* 73: 6715–6720.
18. Matloubian, M., R. J. Concepcion, and R. Ahmed. 1994. $CD4^+$ T cells are required to sustain $CD8^+$ cytotoxic T-cell responses during chronic viral infection. *J. Virol.* 68: 8056–8063.
19. Smyk-Pearson, S., I. A. Tester, J. Klarquist, B. E. Palmer, J. M. Pawlotsky, L. Golden-Mason, and H. R. Rosen. 2008. Spontaneous recovery in acute human hepatitis C virus infection: functional T-cell thresholds and relative importance of CD4 help. *J. Virol.* 82: 1827–1837.
20. Jacobson, S., J. S. Reuben, R. D. Streilein, and T. J. Palker. 1991. Induction of $CD4^+$, human T lymphotropic virus type-1-specific cytotoxic T lymphocytes from patients with HAM/TSP: recognition of an immunogenic region of the gp46 envelope glycoprotein of human T lymphotropic virus type-1. *J. Immunol.* 146: 1155–1162.
21. Kitze, B., K. Usuku, Y. Yamano, S. Yashiki, M. Nakamura, T. Fujiyoshi, S. Izumo, M. Osame, and S. Sonoda. 1998. Human $CD4^+$ T lymphocytes recognize a highly conserved epitope of human T lymphotropic virus type 1 (HTLV-1) env gp21 restricted by HLA DRB1*0101. *Clin. Exp. Immunol.* 111: 278–285.
22. Kobayashi, H., T. Ngato, K. Sato, N. Aoki, S. Kimura, Y. Tanaka, H. Aizawa, M. Tateno, and E. Celis. 2006. In vitro peptide immunization of target tax protein human T-cell leukemia virus type 1-specific $CD4^+$ helper T lymphocytes. *Clin. Cancer Res.* 12: 3814–3822.
23. Yamano, Y., B. Kitze, S. Yashiki, K. Usuku, T. Fujiyoshi, T. Kaminagayoshi, K. Unoki, S. Izumo, M. Osame, and S. Sonoda. 1997. Preferential recognition of synthetic peptides from HTLV-I gp21 envelope protein by HLA-DRB1 alleles associated with HAM/TSP (HTLV-I-associated myelopathy/tropical spastic paraparesis). *J. Neuroimmunol.* 76: 50–60.
24. Goon, P. K., T. Igakura, E. Hanon, A. J. Mosley, A. Barfield, A. L. Barnard, L. Kaftantzi, Y. Tanaka, G. P. Taylor, J. N. Weber, and C. R. Bangham. 2004. Human T cell lymphotropic virus type I (HTLV-I)-specific $CD4^+$ T cells: immunodominance hierarchy and preferential infection with HTLV-I. *J. Immunol.* 172: 1735–1743.
25. Toulza, F., A. Heaps, Y. Tanaka, G. P. Taylor, and C. R. Bangham. 2008. High frequency of $CD4^+FoxP3^+$ cells in HTLV-1 infection: inverse correlation with HTLV-1-specific CTL response. *Blood* 111: 5047–5053.
26. Satou, Y., J. Yasunaga, M. Yoshida, and M. Matsuoka. 2006. HTLV-I basic leucine zipper factor gene mRNA supports proliferation of adult T cell leukemia cells. *Proc. Natl. Acad. Sci. USA* 103: 720–725.
27. Sugata, K., Y. Satou, J. Yasunaga, H. Hara, K. Ohshima, A. Utsunomiya, M. Mitsuyama, and M. Matsuoka. 2012. HTLV-1 bZIP factor impairs cell-mediated immunity by suppressing production of Th1 cytokines. *Blood* 119: 434–444.
28. Iwasaki, Y., Y. Ohara, I. Kobayashi, and S. Akizuki. 1992. Infiltration of helper/inducer T lymphocytes heralds central nervous system damage in human T-cell leukemia virus infection. *Am. J. Pathol.* 140: 1003–1008.
29. Umehara, F., S. Izumo, M. Nakagawa, A. T. Ronquillo, K. Takahashi, K. Matsumuro, E. Sato, and M. Osame. 1993. Immunocytochemical analysis of the cellular infiltrate in the spinal cord lesions in HTLV-I-associated myelopathy. *J. Neuropathol. Exp. Neurol.* 52: 424–430.
30. Umehara, F., S. Izumo, A. T. Ronquillo, K. Matsumuro, E. Sato, and M. Osame. 1994. Cytokine expression in the spinal cord lesions in HTLV-I-associated myelopathy. *J. Neuropathol. Exp. Neurol.* 53: 72–77.
31. Kurihara, K., Y. Shimizu, A. Takamori, N. Harashima, M. Noji, T. Masuda, A. Utsunomiya, J. Okamura, and M. Kannagi. 2006. Human T-cell leukemia virus type-I (HTLV-I)-specific T-cell responses detected using three-divided glutathione-*S*-transferase (GST)-Tax fusion proteins. *J. Immunol. Methods* 313: 61–73.
32. Harashima, N., R. Tanosaki, Y. Shimizu, K. Kurihara, T. Masuda, J. Okamura, and M. Kannagi. 2005. Identification of two new HLA-A*1101-restricted tax epitopes recognized by cytotoxic T lymphocytes in an adult T-cell leukemia patient after hematopoietic stem cell transplantation. *J. Virol.* 79: 10088–10092.
33. Rammensee, H. G., T. Friede, and S. Stevanoviíc. 1995. MHC ligands and peptide motifs: first listing. *Immunogenetics* 41: 178–228.
34. Hanon, E., S. Hall, G. P. Taylor, M. Saito, R. Davis, Y. Tanaka, K. Usuku, M. Osame, J. N. Weber, and C. R. Bangham. 2000. Abundant tax protein expression in $CD4^+$ T cells infected with human T-cell lymphotropic virus type I (HTLV-I) is prevented by cytotoxic T lymphocytes. *Blood* 95: 1386–1392.
35. Richardson, J. H., A. J. Edwards, J. K. Cruickshank, P. Rudge, and A. G. Dalgleish. 1990. In vivo cellular tropism of human T-cell leukemia virus type 1. *J. Virol.* 64: 5682–5687.
36. Sakai, J. A., M. Nagai, M. B. Brennan, C. A. Mora, and S. Jacobson. 2001. In vitro spontaneous lymphoproliferation in patients with human T-cell lymphotropic virus type I-associated neurologic disease: predominant expansion of $CD8^+$ T cells. *Blood* 98: 1506–1511.
37. Elovaara, I., S. Koenig, A. Y. Brewah, R. M. Woods, T. Lehky, and S. Jacobson. 1993. High human T cell lymphotropic virus type 1 (HTLV-1)-specific precursor cytotoxic T lymphocyte frequencies in patients with HTLV-1-associated neurological disease. *J. Exp. Med.* 177: 1567–1573.
38. Kannagi, M., H. Shida, H. Igarashi, K. Kuruma, H. Murai, Y. Aono, I. Maruyama, M. Osame, T. Hattori, H. Inoko, et al. 1992. Target epitope in the Tax protein of human T-cell leukemia virus type I recognized by class I major histocompatibility complex-restricted cytotoxic T cells. *J. Virol.* 66: 2928–2933.
39. Pique, C., A. Ureta-Vidal, A. Gessain, B. Chancerel, O. Gout, R. Tamouza, F. Agis, and M. C. Dokhélar. 2000. Evidence for the chronic in vivo production of human T cell leukemia virus type I Rof and Tof proteins from cytotoxic T lymphocytes directed against viral peptides. *J. Exp. Med.* 191: 567–572.
40. Sundaram, R., Y. Sun, C. M. Walker, F. A. Lemonnier, S. Jacobson, and P. T. Kaumaya. 2003. A novel multivalent human CTL peptide construct elicits robust cellular immune responses in HLA-A*0201 transgenic mice: implications for HTLV-1 vaccine design. *Vaccine* 21: 2767–2781.
41. Vollers, S. S., and L. J. Stern. 2008. Class II major histocompatibility complex tetramer staining: progress, problems, and prospects. *Immunology* 123: 305–313.
42. Sabatino, J. J., Jr., J. Huang, C. Zhu, and B. D. Evavold. 2011. High prevalence of low affinity peptide-MHC II tetramer-negative effectors during polyclonal $CD4^+$ T cell responses. *J. Exp. Med.* 208: 81–90.
43. Goulder, P. J., A. K. Sewell, D. G. Lalloo, D. A. Price, J. A. Whelan, J. Evans, G. P. Taylor, G. Luzzi, P. Giangrande, R. E. Phillips, and A. J. McMichael. 1997. Patterns of immunodominance in HIV-1-specific cytotoxic T lymphocyte responses in two human histocompatibility leukocyte antigens (HLA)-identical siblings with HLA-A*0201 are influenced by epitope mutation. *J. Exp. Med.* 185: 1423–1433.
44. Nowak, M. A., R. M. May, R. E. Phillips, S. Rowland-Jones, D. G. Lalloo, S. McAdam, P. Klenerman, B. Köppe, K. Sigmund, C. R. Bangham, et al. 1995. Antigenic oscillations and shifting immunodominance in HIV-1 infections. *Nature* 375: 606–611.
45. Goulder, P. J., M. A. Altfeld, E. S. Rosenberg, T. Nguyen, Y. Tang, R. L. Eldridge, M. M. Addo, S. He, J. S. Mukherjee, M. N. Phillips, et al. 2001. Substantial differences in specificity of HIV-specific cytotoxic T cells in acute and chronic HIV infection. *J. Exp. Med.* 193: 181–194.
46. Wherry, E. J., J. N. Blattman, K. Murali-Krishna, R. van der Most, and R. Ahmed. 2003. Viral persistence alters CD8 T-cell immunodominance and tissue distribution and results in distinct stages of functional impairment. *J. Virol.* 77: 4911–4927.
47. Jeffery, K. J., K. Usuku, S. E. Hall, W. Matsumoto, G. P. Taylor, J. Procter, M. Bunce, G. S. Ogg, K. I. Welsh, J. N. Weber, et al. 1999. HLA alleles de-

termine human T-lymphotropic virus-I (HTLV-I) proviral load and the risk of HTLV-I-associated myelopathy. *Proc. Natl. Acad. Sci. USA* 96: 3848–3853.
48. Sabouri, A. H., M. Saito, K. Usuku, S. N. Bajestan, M. Mahmoudi, M. Forughipour, Z. Sabouri, Z. Abbaspour, M. E. Goharjoo, E. Khayami, et al. 2005. Differences in viral and host genetic risk factors for development of human T-cell lymphotropic virus type 1 (HTLV-1)-associated myelopathy/tropical spastic paraparesis between Iranian and Japanese HTLV-1-infected individuals. *J. Gen. Virol.* 86: 773–781.
49. Kurihara, K., N. Harashima, S. Hanabuchi, M. Masuda, A. Utsunomiya, R. Tanosaki, M. Tomonaga, T. Ohashi, A. Hasegawa, T. Masuda, et al. 2005. Potential immunogenicity of adult T cell leukemia cells in vivo. *Int. J. Cancer* 114: 257–267.
50. Aubert, R. D., A. O. Kamphorst, S. Sarkar, V. Vezys, S. J. Ha, D. L. Barber, L. Ye, A. H. Sharpe, G. J. Freeman, and R. Ahmed. 2011. Antigen-specific CD4 T-cell help rescues exhausted CD8 T cells during chronic viral infection. *Proc. Natl. Acad. Sci. USA* 108: 21182–21187.

HTLV-1 bZIP Factor Induces Inflammation through Labile Foxp3 Expression

Nanae Yamamoto-Taguchi[1], Yorifumi Satou[1], Paola Miyazato[1], Koichi Ohshima[2], Masanori Nakagawa[3], Koko Katagiri[4], Tatsuo Kinashi[5], Masao Matsuoka[1]*

1 Laboratory of Virus Control, Institute for Virus Research, Kyoto University, Kyoto, Japan, **2** Department of Pathology, School of Medicine, Kurume University, Fukuoka, Japan, **3** Department of Neurology, Graduate School of Medical Science, Kyoto Prefectural University of Medicine, Kyoto, Japan, **4** Department of Biosciences, School of Science, Kitasato University, Kanagawa, Japan, **5** Department of Molecular Genetics, Institute of Biomedical Science, Kansai Medical University, Osaka, Japan

Abstract

Human T-cell leukemia virus type 1 (HTLV-1) causes both a neoplastic disease and inflammatory diseases, including HTLV-1-associated myelopathy/tropical spastic paraparesis (HAM/TSP). The HTLV-1 basic leucine zipper factor (HBZ) gene is encoded in the minus strand of the proviral DNA and is constitutively expressed in infected cells and ATL cells. HBZ increases the number of regulatory T (Treg) cells by inducing the *Foxp3* gene transcription. Recent studies have revealed that some $CD4^+Foxp3^+$ T cells are not terminally differentiated but have a plasticity to convert to other T-cell subsets. Induced Treg (iTreg) cells tend to lose Foxp3 expression, and may acquire an effector phenotype accompanied by the production of inflammatory cytokines, such as interferon-γ (IFN-γ). In this study, we analyzed a pathogenic mechanism of chronic inflammation related with HTLV-1 infection via focusing on HBZ and Foxp3. Infiltration of lymphocytes was observed in the skin, lung and intestine of HBZ-Tg mice. As mechanisms, adhesion and migration of HBZ-expressing $CD4^+$ T cells were enhanced in these mice. $Foxp3^-CD4^+$ T cells produced higher amounts of IFN-γ compared to those from non-Tg mice. Expression of Helios was reduced in Treg cells from HBZ-Tg mice and HAM/TSP patients, indicating that iTreg cells are predominant. Consistent with this finding, the conserved non-coding sequence 2 region of the *Foxp3* gene was hypermethylated in Treg cells of HBZ-Tg mice, which is a characteristic of iTreg cells. Furthermore, Treg cells in the spleen of HBZ-transgenic mice tended to lose Foxp3 expression and produced an excessive amount of IFN-γ, while Foxp3 expression was stable in natural Treg cells of the thymus. HBZ enhances the generation of iTreg cells, which likely convert to $Foxp3^-$ T cells producing IFN-γ. The HBZ-mediated proinflammatory phenotype of $CD4^+$ T cells is implicated in the pathogenesis of HTLV-1-associated inflammation.

Citation: Yamamoto-Taguchi N, Satou Y, Miyazato P, Ohshima K, Nakagawa M, et al. (2013) HTLV-1 bZIP Factor Induces Inflammation through Labile Foxp3 Expression. PLoS Pathog 9(9): e1003630. doi:10.1371/journal.ppat.1003630

Editor: Jeremy Luban, University of Massachusetts Medical School, United States of America

Received April 11, 2013; **Accepted** August 1, 2013; **Published** September 19, 2013

Funding: This study was supported by a Grant-in-Aid for Scientific Research from the Ministry of Education, Science, Sports, and Culture of Japan (22114003), and a grant from SENSHIN medical research foundation, and a grant from Japan Leukaemia Research Fund to MM; a grant from Takeda Science Foundation; and a grant from Naito Foundation to YS. The funders had no role in study design, data collection and analysis, decision to publish, or preparation of the manuscript.

Competing Interests: The authors have declared that no competing interests exist.

* E-mail: mmatsuok@virus.kyoto-u.ac.jp

Introduction

Human T-cell leukemia virus type 1 (HTLV-1) is known to be the causal agent of a neoplastic disease of $CD4^+$ T cells, adult T-cell leukemia (ATL) [1]. In addition, this virus perturbs the host immune system, causing inflammatory diseases and immunodeficiency. Inflammatory diseases associated with HTLV-1 include HTLV-1-associated myelopathy/tropical spastic paraparesis (HAM/TSP) [2,3], uveitis [4,5], alveolitis [6], infective dermatitis [7] and myositis [8]. Increased expression of inflammatory cytokines and immune response to the Tax antigen has been proposed as mechanisms of these inflammatory diseases [9]. However, the detailed mechanisms of inflammation remain elusive.

The *HTLV-1 bZIP factor* (*HBZ*) gene is encoded in the minus strand of the provirus and consistently expressed in ATL cases and HTLV-1-infected individuals [10]. *In vitro* and *in vivo* experiments have shown that the *HBZ* gene promotes the proliferation of T cells and increases their number [10,11]. Recently, we reported that HBZ transgenic (HBZ-Tg) mice develop both T-cell lymphomas and inflammatory diseases [12]. In HBZ-Tg mice, we found that the number of $CD4^+$ T cells expressing Foxp3, a master molecule for regulatory T (Treg) cells, was remarkably increased. HBZ induces transcription of the *Foxp3* gene via interaction with Smad2/3 and a co-activator, p300, resulting in an increased number of $Foxp3^+$ T cells [13]. Concurrently, HBZ interacts with Foxp3 and decreases the immune suppressive function [12]. This interaction could be a mechanism of the inflammatory phenotype observed in HBZ-Tg mice. However, detailed mechanisms to induce inflammation by HBZ remain unsolved.

Treg cells suppress excessive immune responses, and control the homeostasis of the immune system [14]. Foxp3 is considered a marker of Treg cells, yet several lines of evidence have shown that there is heterogeneity within $Foxp3^+$cells [15]. Natural Treg (nTreg) cells are generated in the thymus while induced Treg (iTreg) cells are induced in the peripheral lymphoid organs. It has been reported that Treg cells that have lostFoxp3 expression (exFoxp3 T cells) produce interferon-γ (IFN-γ), indicating that$Foxp3^+$ Treg cells are not terminally differentiated cells but

Author Summary

Viral infection frequently induces tissue inflammation in the host. HTLV-1 infection is associated with chronic inflammation in the CNS, skin, and lung, but the inflammatory mechanism is not fully understood yet. Since HTLV-1 directly infects $CD4^+$ T cells, central player of the host immune regulation, HTLV-1 should modulate the host immune response not only via viral antigen stimulation but also via $CD4^+$ T-cell-mediated immune deregulation. It has been reported that $Foxp3^+CD4^+$ T cells are increased in HTLV-1 infection. It remains a central question in HTLV-1 pathogenesis why HTLV-1 induces inflammation despite of increase of $FoxP3^+$ cells, which generally possess immune suppressive function. We have elucidated here that most of the increased $Foxp3^+$ cells in HBZ-Tg mice or HAM/TSP patients is not thymus-derived naturally occurring Treg cells but induced Treg cells. Since the iTreg cells are prone to lose FoxP3 expression and then become cytokine-producing cells, the increase of iTreg cells could serve as a source of proinflammatory $CD4^+$ T cells. Thus HTLV-1 causes abnormal $CD4^+$ T-cell differentiation by expressing HBZ, which should play a crucial role in chronic inflammation related with HTLV-1. This study has provided new insights into the mechanism of chronic inflammation accompanied with viral infection.

susceptible to conversion into effector T cells according to their environment [16]. Recently, Miyao et al. have reported that $Foxp3^+$ T cells induced by activation exhibit transient Foxp3 expression, and become exFoxp3 T cells [17]. Even though the plasticity of Treg cells remains controversial [18], these reports suggest that $Foxp3^+$ T cells possess not only suppressive function but also proinflammatory attributes.

In this study, we found that iTreg cells increased in HBZ-Tg mice and that Treg cells of HBZ-Tg mice tend to lose Foxp3 expression, leading to increased IFN-γ-expressing proinflammatory cells. Cell adhesion and migration are enhanced in $CD4^+$ T cells of HBZ-Tg mice. Thus, these HBZ-mediated abnormalities of CD4 T cells play critical roles in inflammatory diseases caused by HTLV-1.

Results

HBZ-Tg mice spontaneously develop inflammation

We have reported that HBZ-Tg mice develop both T-cell lymphoma and inflammatory diseases including dermatitis and alveolitis [12]. To further study the inflammatory changes affecting HBZ-Tg mice, we analyzed various tissues and organs in detail. In HBZ-Tg mice, moderate lymphoid cell infiltration was detected in the peri-bronchial space of the lung (Figure 1A), the peri-follicular area of the skin (Figure 1B), the mucosa of the small intestine (Figure 1C), and the mucosa of the colon (Figure 1D). Meanwhile, there was no obvious evidence of inflammation in liver, kidney or spinal cord. In non-Tg littermates, infiltration of lymphoid cells was not observed in skin, lung or intestine. These findings suggest the inflammatory involvement of multiple tissues and organs in HBZ-Tg mice.

Enhanced cell adhesion and migration of HBZ-Tg $CD4^+$ T cells

Infiltration of lymphocytes into various tissues suggests that the lymphocytes of HBZ-Tg mice have increased adhesive ability. We first studied the expression of LFA-1, which is a heterodimer of CD11a and CD18. As shown in Figure 2A, both CD11a and

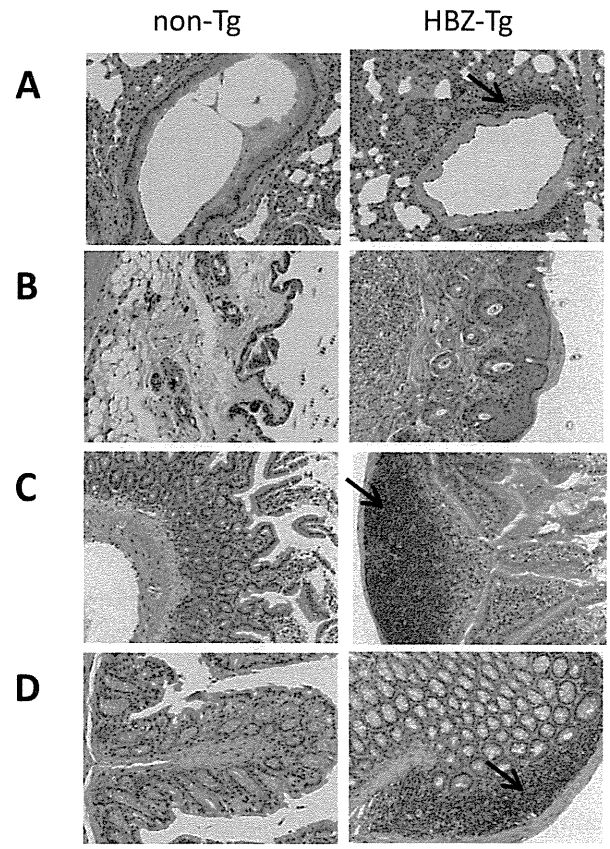

Figure 1. Histopathology of mouse inflammatory tissue. Hematoxylin and eosin staining of lung (A), skin (B), small intestine (C) and large intestine (D) from non-Tg littermate mice (left) or HBZ-Tg mice (right). Original magnification, ×10. Arrows indicate massive infiltration of lymphocytes.
doi:10.1371/journal.ppat.1003630.g001

CD18 were upregulated on HBZ-Tg $CD4^+$ T cells of spleen, lung and lymph nodes compared with $CD4^+$ T cells from non-Tg mice. In addition, the expression of CD103 (alpha E integrin) on HBZ-Tg $CD4^+$ T cells was also higher than that on non-Tg $CD4^+$ T cells. These findings suggest an increased adhesive capability of $CD4^+$ T cells in HBZ-Tg mice. Immunohistochemical analyses of lung and intestine of HBZ-Tg mice confirmed increased expression of these molecules, particularly CD18 (Figure 2B, C).

Expression of CD11a, CD18 and CD103 was also studied in HAM/TSP patients. In addition to healthy donors, we analyzed expression of these molecules on HTLV-1 infected cells that are identified using anti-Tax antibody. As shown in Figure 2D, CD11a and CD18 expression of $CD4^+Tax^+$ T cells was upregulated compared with $CD4^+$ T cells from healthy donors and $CD4^+Tax^-$ T cells of HAM/TSP patients while expression of CD103 was not different among these cells. These results show that enhanced expression of LFA-1 is also observed in HTLV-1 infected cells in HAM/TSP patients.

We next investigated adhesion of $CD4^+$ T cells to ICAM-1, since ICAM-1 is critical for lymphocyte migration and adhesion to vascular epithelial cells in an inflammatory lesion. We isolated $CD4^+$ T cells from non-Tg or HBZ-Tg splenocytes, placed them on ICAM-1-coated 96-well plates, and evaluated cell adhesion activity to ICAM-1. $CD4^+$ T cells from HBZ-Tg mice showed increased adhesion in the absence of stimulation, while no difference was found when cells were stimulated by anti-CD3 antibody (Figure 3A). Furthermore, we

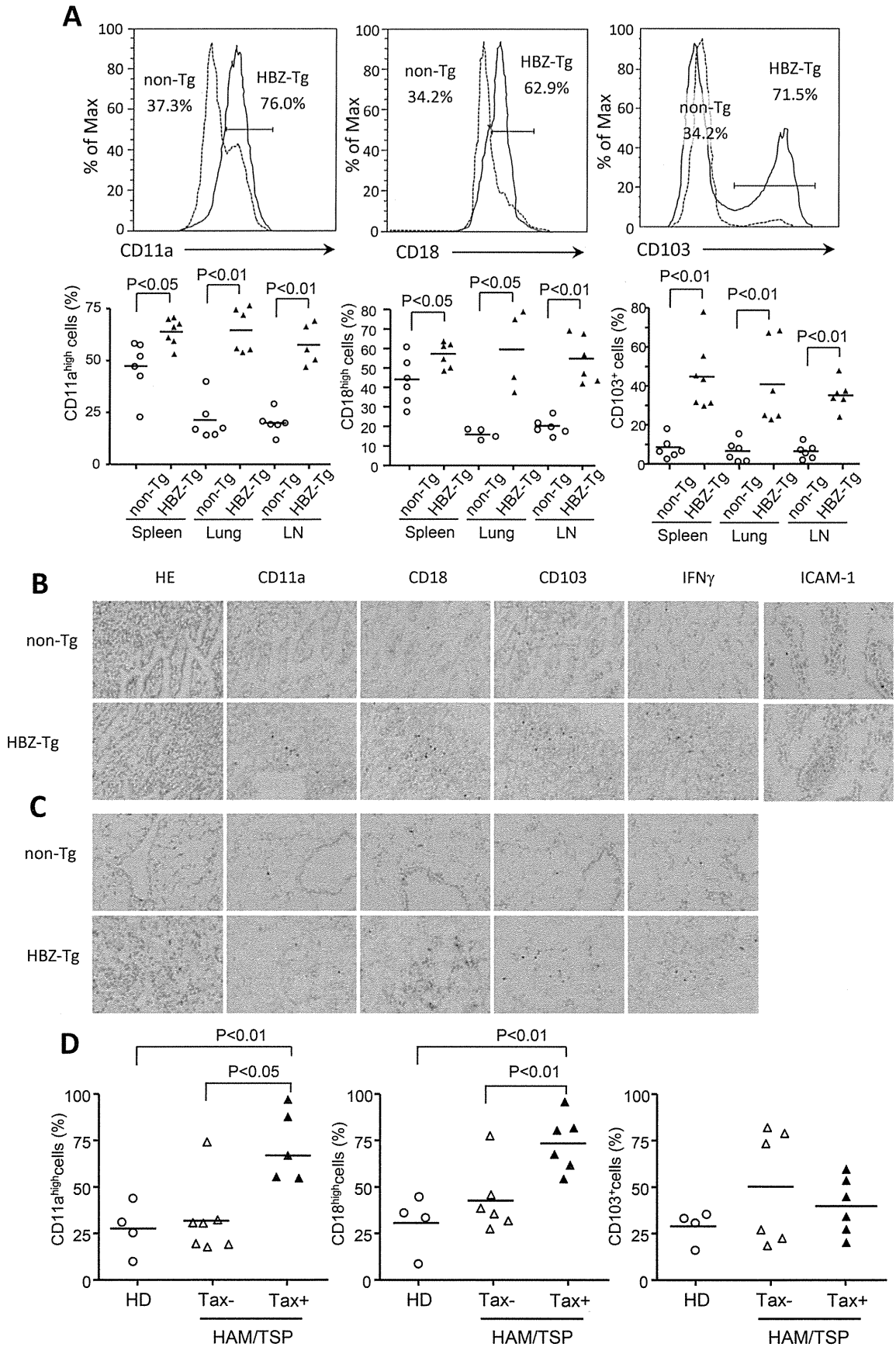
A
non-Tg
37.3%
HBZ-Tg
76.0%
% of Max
CD11a
non-Tg
34.2%
HBZ-Tg
62.9%
CD18
non-Tg
34.2%
HBZ-Tg
71.5%
CD103
CD11a^high cells (%)
CD18^high cells (%)
CD103+ cells (%)
P<0.05
P<0.01
non-Tg
HBZ-Tg
Spleen
Lung
LN
B
HE
CD11a
CD18
CD103
IFNγ
ICAM-1
non-Tg
HBZ-Tg
C
non-Tg
HBZ-Tg
D
CD11a^high cells (%)
CD18^high cells (%)
CD103+ cells (%)
P<0.01
P<0.05
HD
Tax-
Tax+
HAM/TSP

Figure 2. Expression of CD11a, CD18 and CD103 in CD4$^+$T cells from spleen, lung and LN cells isolated from HBZ-Tg mice. (A) The expression of CD11a, CD18 and CD103 in CD4$^+$ T cells from non-Tg (dashed line) and HBZ-Tg (solid line) mice was analyzed by flow cytometry. Histograms from one representative mouse splenocytes of each group are shown (top panels). The bottom panel shows the results of 4 or 6 mice in each group, each symbol representing an individual mouse. The small horizontal lines indicate the mean. Frozen sections of intestine (B) and lung (C) of non-Tg and HBZ-Tg mice were stained with HE and the indicated antibodies. Original magnification is ×20. Results from one representative mouse of each group are shown. (D) CD11a, CD18 and CD103 expressions are shown on CD4$^+$ cells from HDs, CD4$^+$Tax$^-$ and CD4$^+$Tax$^+$ cells from HAM/TSP patients.
doi:10.1371/journal.ppat.1003630.g002

evaluated the migration activity of CD4$^+$ T cells on ICAM-1-coated plates. To induce cell migration, we stimulated CD4$^+$ T cells with CCL22 as reported previously [19]. Cell migration of HBZ-Tg CD4$^+$ T cells was also increased compared with migration of non-Tg CD4$^+$ T cells (Figure 3B). These results demonstrate an infiltrative phenotype of CD4$^+$ T cells in HBZ-Tg mice.

Infiltration of LFA-1 expressing T cells into various tissues suggests that ICAM-1 expression is enhanced. Indeed, expression of ICAM-1 was increased in intestine of HBZ-Tg mice (Figure 2B). Enhanced migration of CD4$^+$ T cells suggests involvement of chemokine(s)-chemokine receptor for HBZ-Tg mice. We analyzed expression of chemokine receptors on CD4$^+$ T cells of HBZ-Tg mice. As shown in Figure 3C, CXCR3 expression of CD4$^+$ splenocytes was increased while expression of CCR5 and CCR7 were not different compared with control mice (Figure S1). CXCR3 expression of CD4$^+$ T cells was upregulated in both lung and lymph node (Figure 3C). Although the ligands for CXCR3, CXCL9 and CXCL10, were not increased in the sera of HBZ-Tg

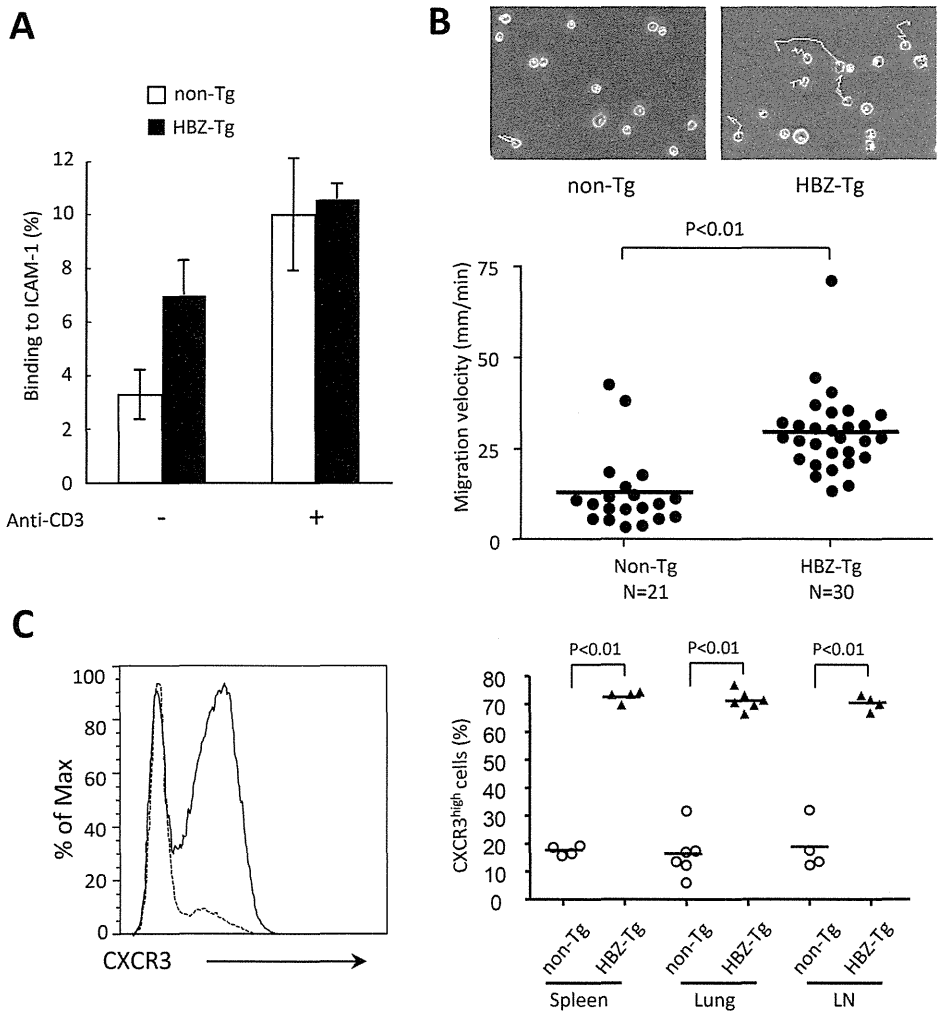

Figure 3. Enhanced capacity for cell adhesion and migration of CD4$^+$splenocytes isolated from HBZ-Tg mice. (A) Assays of cell adhesion to mouse ICAM-1 were performed using purified mouse CD4$^+$splenocytes of HBZ-Tg or non-Tg mice. Results shown are means ± s.d. of triplicate wells. (B) Random CD4$^+$ mouse splenocyte migration was recorded at 37°C with a culture dish system for live-cell microscopy. Phase-contrast images were taken every 15 seconds for 10 min. The cells were traced and migration velocity was calculated. Each dot represents the velocity of an individual cell, and bars indicate the mean (n = 21 for non-Tg, n = 30 for HBZ-Tg). Statistical analyses were performed using an unpaired, two-tailed Student *t*-test. (C) Representative histograms of CXCR3 expression in CD4$^+$ T cells from non-Tg (dashed line) and HBZ-Tg (solid line) mice (left) and cumulative results from 4 or 6 mice are shown in the graph (right) for spleen, lung and lymph node. Each symbol represents an individual mouse; small horizontal lines indicate the mean.
doi:10.1371/journal.ppat.1003630.g003

mice (Figure S1), CXCR3 might be implicated in infiltration of $CD4^+$ T cells.

Pro-inflammatory cytokine production by $CD4^+$ T cells in the HBZ-Tg mice

To elucidate the mechanism of the pro-inflammatory phenotype observed in HBZ-Tg mice, we investigated cytokine production in $CD4^+$ T cells of the spleen. After stimulation by PMA/ionomycin, production of IFN-γ was increased in $CD4^+$ T cells while that of TNF-α was suppressed (Figure 4A). There were no significant differences between HBZ-Tg mice and non-Tg mice in IL-2, IL-4 and IL-17 production by $CD4^+$ T cells. We have reported that the number of $Foxp3^+CD4^+$ Treg cells is increased in HBZ-Tg mice. Therefore, we simultaneously stained both intracellular cytokines and Foxp3 to distinguish the cytokine production of $CD4^+Foxp3^-$ T cells from that of $CD4^+Foxp3^+$ T cells. Production of TNF-α, IL-17 and IL-2 was slightly increased in $CD4^+Foxp3^+$ T cells of HBZ-Tg mice (Figure 4B, C). Since Foxp3 suppresses production of cytokines [19], and HBZ impairs function of Foxp3 [12], HBZ-mediated impairment of Foxp3 function might be a mechanism of this increased expression of these cytokines. However, TNF-α production was suppressed in $CD4^+$ $Foxp3^-$ T cells and total $CD4^+$ T cells (Figure 4A, C). In particular, IFN-γ production of splenic $CD4^+Foxp3^-$ T cells from HBZ-Tg mice was remarkably increased compared with those from non-Tg mice (Figure 4B). We also studied IFN-γ production in $CD4^+$ T cells of

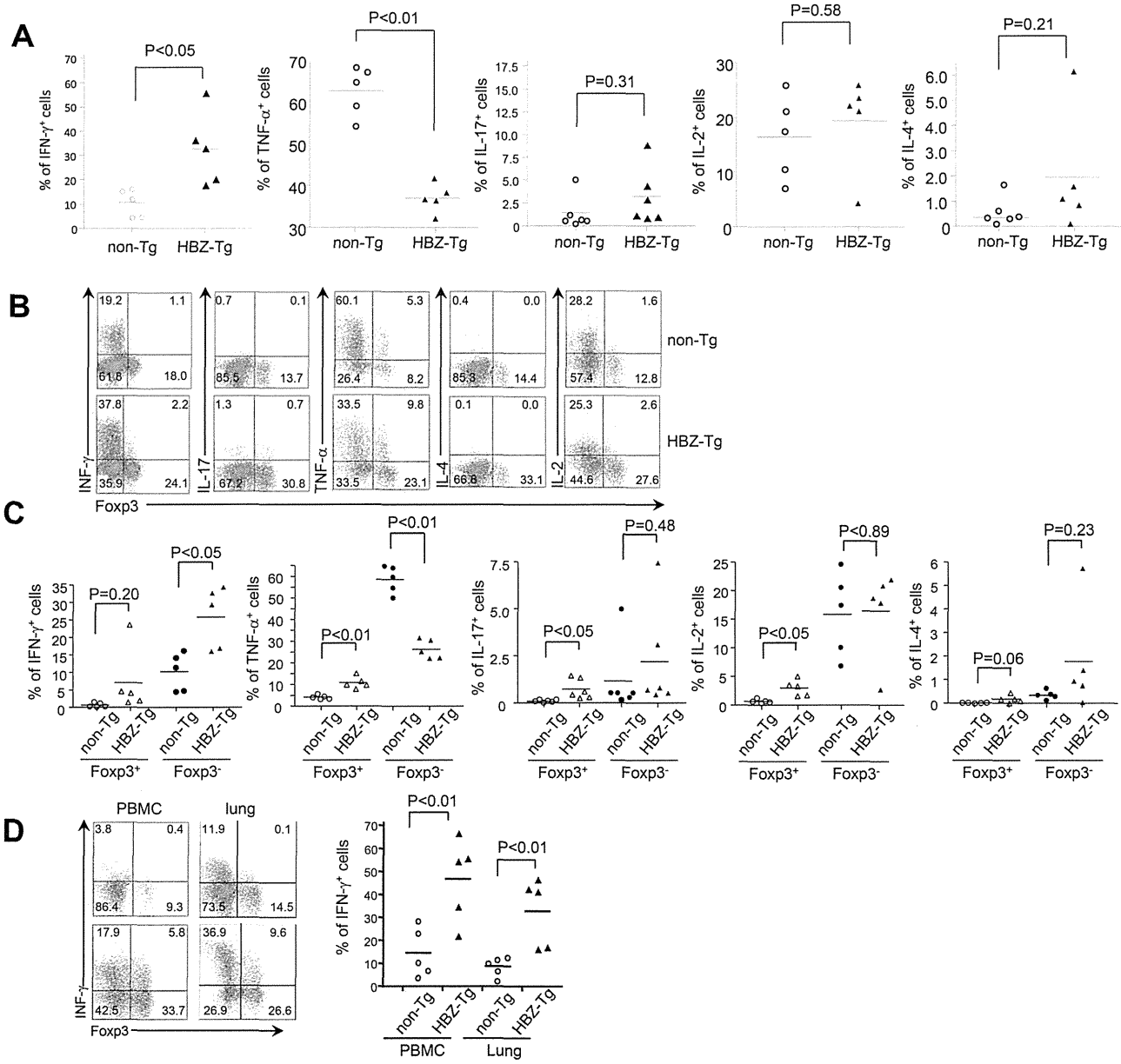

Figure 4. Production of cytokines in HBZ-Tg mice. (A) Splenocytes of HBZ-Tg mice or non-Tg mice were stimulated with PMA/ionomycin and protein transport inhibitor for 4 h. IFN-γ, IL-17, TNF-α, IL-4 or IL-2 production was analyzed in $CD4^+$ T cells by flow cytometry. (B) Cytokine production was analyzed along with Foxp3 expression. (C) Production of cytokines was shown in $CD4^+Foxp3^+$ T cells and $CD4^+Foxp3^-$ T cells. (D) IFN-γ and Foxp3 expression gated on $CD4^+$ T cells from PBMC or cells isolated from the lungs were analyzed by flow cytometry. Percentage of IFN-γ^+ cells in $CD4^+$ splenocytes, PBMC and lung cells. Each symbol represents an individual mouse; small horizontal lines indicate the mean.
doi:10.1371/journal.ppat.1003630.g004

PBMCs and lung-infiltrating lymphocytes. The production of IFN-γ was remarkably increased in PBMC and lung from HBZ-Tg mice (Figure 4D). Taken together, these results suggest that increased IFN-γ production, especially in $CD4^+Foxp3^-$ T cells, is related to the chronic inflammation observed in HBZ-Tg mice. Immunohistochemical analyses also showed that IFN-γ production was increased in both lung and intestine of HBZ-Tg mice (Figure 2B, C).

Increased number of induced Treg cells in HBZ-Tg mice

We have reported that HBZ enhances the transcription of the *Foxp3* gene in cooperation with TGF-ß, leading to an increased number of Treg cells *in vivo* [12,13]. Two types of Treg cells have been reported: natural Treg (nTreg) cells and induced Treg (iTreg) cells in $CD4^+Foxp3^+$ cells. The expression of Helios, a member of the Ikaros family of transcription factors, is considered a marker of nTreg cells [20]. To determine which Treg cell population is increased in HBZ-Tg mice, we analyzed the expression of Helios. Expression of Helios in $CD4^+Foxp3^+$ T cells in HBZ-Tg mice was lower than that in non-Tg mice (Figure 5A, C), suggesting that the number of iTreg cells is increased in HBZ-Tg mice. A higher proportion of $CD4^+Foxp3^+Helios^{low}$ cells were found in the lungs of HBZ-Tg mice (Figure S2). Next, we analyzed the expression of Helios in Treg cells from HAM/TSP patients. As shown in Figure 5 B and D, Helios expression of Treg cells in HAM/TSP patients was lower than that of Treg cells in healthy controls. We also analyzed Helios expression in $Foxp3^+$ T (nTreg) cells of the thymus. The level of Helios expression in nTreg cells in HBZ-Tg mice was equivalent to that of non-Tg mice (Figure S3). These data collectively suggest that the iTreg cell population is increased not only in HBZ-Tg mice, but also in HAM/TSP patients.

Recent studies have reported that Helios expression is not always associated with nTreg cells [21–23]. A previous study reported that conserved non-coding DNA sequence (CNS) elements in the *Foxp3* locus play an important role in the induction and maintenance of *Foxp3* gene expression [24]. Among these elements, CNS2, methylated in iTreg cells, was suggested to be responsible for the lack of stable expression of Foxp3 in these cells [24]. This region is not methylated in Helios- nTreg cells, indicating that unmethylation of this region is a suitable marker of nTreg cells [21]. Therefore, we sorted the Treg fraction from HBZ-Tg or non-Tg mice splenocytes, extracted genomic DNA, and determined the DNA methylation status in the CNS2 region of the *Foxp3* gene. The results revealed

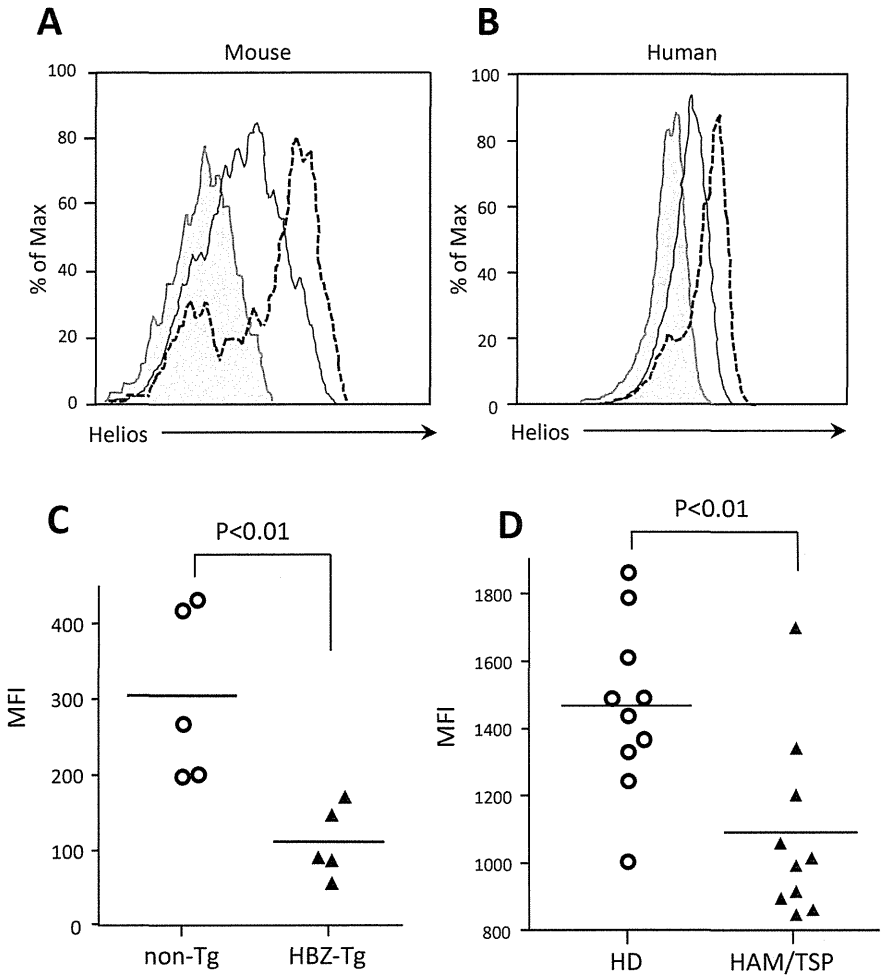

Figure 5. Helios expression in HBZ-Tg mice and HAM/TSP patients. (A) Expression of Helios in $CD4^+Foxp3^+$ cells of HBZ-Tg mice (solid line), non-Tg mice (dashed line) and isotype control (filled histogram). (B) Intracellular Helios expression in gated $CD4^+$ T cells from HAM/TSP patients (solid line), healthy donors (dashed line), or isotype control (filled histogram). One representative histogram for each group is shown. (C) Results from 5 non-Tg and 5 HBZ-Tg mice are shown. (D) Comparison of Helios expression in $CD4^+FoxP3^+$PBMC's from 10 HAM/TSP patients and 10 healthy donors. Each symbol represents the value for an individual subject. Statistical analyses were performed using an unpaired, two-tailed Student *t*-test.
doi:10.1371/journal.ppat.1003630.g005

that in HBZ-Tg $CD4^+Foxp3^+$ T cells, the CNS2 region had a higher methylation status than in non-Tg $CD4^+Foxp3^+$ cells (Figure 6), indicating that the increase in $CD4^+Foxp3^+$ cells in HBZ-Tg mice indeed mostly consists of iTreg cells.

Foxp3 expression in $CD4^+Foxp3^+$ T cells in HBZ-Tg mice is unstable, leading to the generation of exFoxp3 T cells expressing IFN-γ

Recent studies have revealed that $CD4^+Foxp3^+$ T cells are not terminally differentiated but have the plasticity to convert to other T cell subsets [25]. When Treg cells lose the expression of Foxp3 (exFoxp3 T cells), such cells produce pro-inflammatory cytokines [16]. It has been reported that Foxp3 expression in nTreg cells is stable but that it is not in iTreg cells [15]. These findings suggest that in HBZ-Tg mice, which have greater numbers of iTreg cells as shown in this study, Foxp3 expression in these cells tends to diminish, letting these cells acquire an effector phenotype associated with the production of pro-inflammatory cytokines such as IFN-γ. To investigate this possibility, we sorted Treg cells from the spleens of HBZ-Tg or non-Tg mice based on their expression of CD4, CD25 and GITR; cultured them for 7 days; and analyzed Foxp3 expression by flow cytometry. After 7 days in culture, the percentage of $Foxp3^+$ T cells diminished remarkably in HBZ-Tg mice compared with non-Tg mice (Figure 7A, B). We investigated the production of IFN-γ at this point, and found that it was increased in $Foxp3^-$ T cells from HBZ-Tg mice compared with those from non-Tg mice (Figure 7C). In sharp contrast to this finding, Foxp3 expression of nTreg cells did not change in $CD4^+$ thymocytes of HBZ-Tg mice (Figure 7D). Collectively, these data indicate thatFoxp3 expression in nTreg cells is stable in HBZ-Tg mice, while most of the Treg cells in the periphery are iTreg cells. The enhanced generation of exFoxp3 T cells in the periphery is a

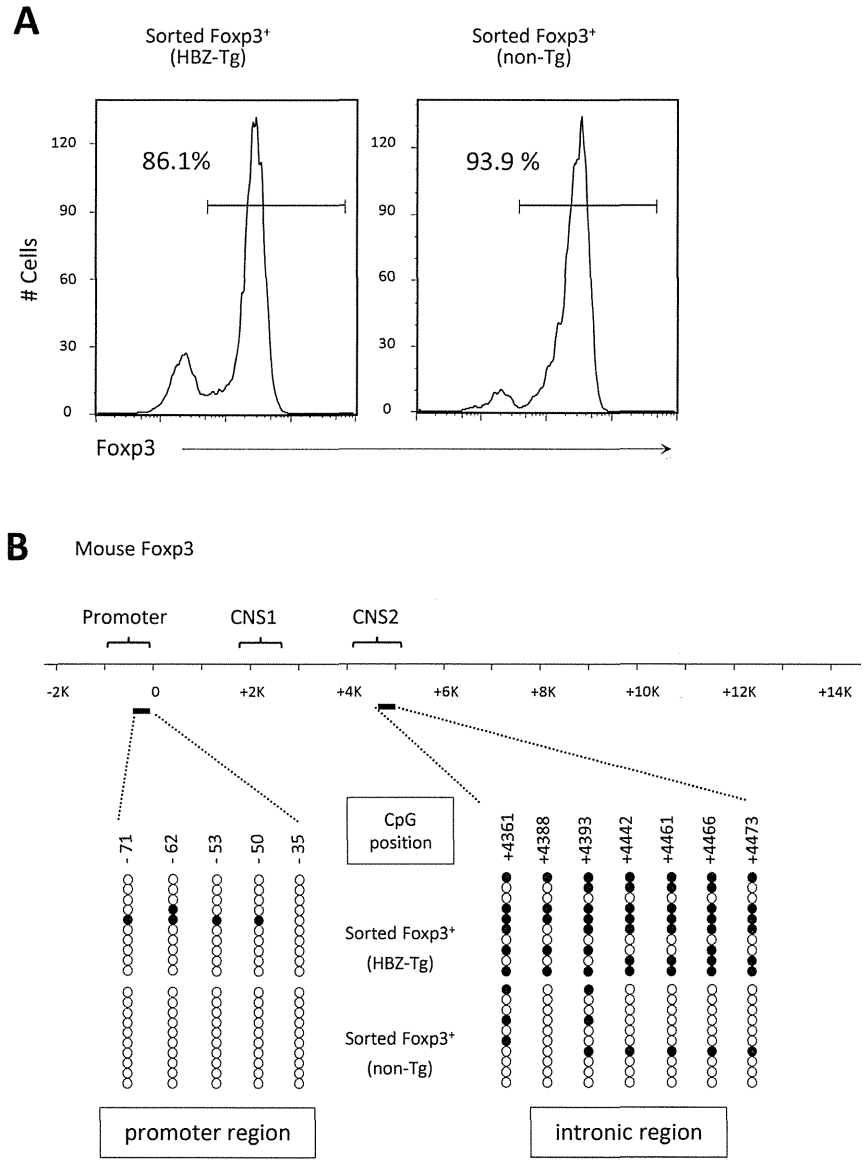

Figure 6. DNA methylation status in the promoter and intronic CpG island region of the *Foxp3* gene. (A) The purity of the isolated Treg cells, sorted from the spleens of male mice, was confirmed by staining the intracellular expression of Foxp3 and analysis by flow cytometry. (B) DNA methylation status in the indicated regions was determined by bisulfite sequencing. Each line represents one analyzed clone; open circles, unmethylated CpGs and filled circles, methylated CpGs.
doi:10.1371/journal.ppat.1003630.g006

possible mechanism of the increase in IFN-γ -producing Foxp3$^-$ T cells in HBZ-Tg mice. We reported that HBZ induced the *Foxp3* gene transcription via interaction with activation of TGF-β/Smad pathway [13]. Reduced expression of Foxp3 in HBZ-Tg CD4$^+$Foxp3$^-$ T cells might be caused by low HBZ expression in that cell population. To investigate this possibility, we analyzed the relationship between HBZ and Foxp3 expression in CD4$^+$ T cells of HBZ-Tg mice. We isolated CD4$^+$CD25$^+$GITR^{high} T cells as Foxp3$^+$ T cells, and CD4$^+$CD25$^-$GITR^{low} T cells as Foxp3$^-$ T cells from HBZ-Tg mice. Although Foxp3+ T cells are contaminated in CD4$^+$CD25$^-$GITR^{low} T cells, level of the Foxp3 gene transcript was much higher in CD4$^+$CD25^{high}GITR^{high} T cells (Figure S4). However, level of *HBZ* transcript was no different among these cells, indicating that level of HBZ expression is not associated with reduced Foxp3 expression.

Discussion

HTLV-1 is a unique human retrovirus with respect to its pathogenesis, since it causes not only a neoplastic disorder, but also various inflammatory diseases. For most viruses, tissue-damaging inflammation associated with chronic viral infection is generally triggered by the immune response against infected cells, which involves both antigen specific and non-specific T cells that produce pro-inflammatory cytokines, chemokines, and other chemical mediators that promote tissue inflammation [26]. However, this study shows that HTLV-1 can induce inflammation by a different mechanism that does not involve an immune response against infected cells, but instead, involves deregulation of CD4$^+$ T-cell differentiation mediated by HBZ. Since transgenic expression of HBZ does not induce an immune response to HBZ protein itself, the inflammation observed in this study is attributed to an intrinsic property of HBZ-expressing cells.

Studies of the pathogenesis of inflammatory diseases related to HTLV-1 are usually focused on HAM/TSP, since it is the most common inflammatory disease caused by this virus [9]. Two different mechanisms of HAM/TSP pathogenesis have been reported: one mechanism involves the immune response to viral antigens, and another mechanism implicates the proinflammatory attributes of HTLV-1-infected cells themselves. Previous studies reported a strong immune response to Tax in HTLV-1-infected individuals [9,27]. In lesions of the spinal cord, CD4$^+$ T cells expressing viral gene transcripts were identified by in situ hybridization [28]. The presence of CTLs targeting Tax in cerebrospinal fluid and lesions in the spinal cord suggest an important role of the immune response and the cytokines produced by CTLs in the pathogenesis of HAM/TSP by HTLV-1 [29]. Those studies showed the involvement of the immune response to Tax in the pathogenesis of HAM/TSP. In addition, cell-autonomous production of proinflammatory cytokines by HTLV-1-infected cells has been reported. HTLV-1-transformed cells produce a variety of cytokines, including IFN-γ, IL-6, TGF-ß, and IL-1α [30]. It was speculated that Tax was responsible for the enhanced production of these cytokines. In this study, we have shown a new role of HBZ in inflammatory diseases. CTLs against HBZ have been reported in HTLV-1 carriers and HAM/TSP patients; this immune response might be involved in inflammation caused by HTLV-1 [31]. However, an immune response to HBZ does not occur in HBZ-Tg mice, indicating that the proinflammatory phenotype of HBZ expressing T cells is sufficient to cause the inflammation.

Does HBZ induce IFN-γ production in CD4$^+$ T cells? HBZ and Tax have contradictory effects on many pathways. For example, Tax activates both the canonical and non-canonical NF-κB pathways, while HBZ suppresses the canonical pathway [32,33]. Conversely, HBZ activates TGF-ß/Smad pathway, while Tax inhibits it [13,34,35]. Tax activates the IFN-γ gene promoter, whereas HBZ suppresses the transcription of the IFN-γ gene through inhibition of AP-1 and NFAT, which are critical for IFN-γ gene transcription [36]. These findings collectively suggest that the enhanced production of IFN-γ is not due to a direct effect of HBZ, but may be attributed to the increased presence exFoxp3 T cells triggered by HBZ as shown in this study. Recent studies reported that exFoxp3 T cells produce higher amount of IFN-γ [17,37]. This indicates that increased production of IFN-γ in exFoxp3 T cells surpasses the suppressive function by HBZ. In this study, HBZ inhibited the production of TNF-α as we reported [36], indicating that enhanced production is specific to IFN-γ. However, it remains unknown how the production of IFN-γ is enhanced in exFoxp3 T cells.

We have shown that the Foxp3$^+$ T cells of HBZ-Tg mice tend to lose Foxp3 expression and change into IFN-γ-producing proinflammatory cells. This observation makes sense in the light of several other studies on Treg cells. It was reported thatFoxp3$^+$ T cells convert to Foxp3$^-$ T cells [37–39]. Recently, Miyao et al. reported that Foxp3 expression of peripheral T cells induced by activation is promiscuous and unstable, leading to conversion to exFoxp3 T cells [17]. Peripheral induced Foxp3$^+$ T cells show lower expression of CD25 and Helios, which corresponds to the phenotype we observed in the Foxp3$^+$ T cells of HBZ-Tg mice. Thus it is likely that HBZ induces unstable Foxp3 expression and generates iTreg cells, which then convert to exFoxp3 T cells with enhanced production of IFN-γ as shown in this study. It has recently been reported that CD4$^+$CD25$^+$CCR4$^+$ T cells in HAM/TSP patients were producing extraordinarily high levels of IFN-γ, when compared to cells of healthy donors. These findings are consistent with those of this study. Importantly, the frequency of these IFN-γ-producing CD4$^+$CD25$^+$CCR4$^+$Foxp3$^-$ T cells was increased and found to be correlated with disease severity in HAM/TSP patients [40]. In addition, it has been reported that HBZ expression is correlated with the severity of HAM/TSP [41]. Thus, the presence of abnormal HBZ-induced IFN-γ-producing cells is a plausible mechanism that leads to inflammation in HAM/TSP patients.

FOXP3 expression is detected in two thirds of ATL cases, suggesting that ATL cells originate from Treg cells in these cases [42,43]. Human FOXP3$^+$ T cells have been divided into three subgroups based on their functions and surface makers: resting Treg cells (rTreg), activated Treg (aTreg) cells, and FOXP3^{low}non-suppressive T cells [44]. Recently, we reported that HTLV-1 infection is frequently detected in Treg cells, which include FOXP3^{low} non-suppressive T cells and FOXP3^{high} activated Treg cells, and concordantly, some ATL cells also belong to the population of FOXP3^{low} non-suppressive T cells [44,45]. This suggests that HTLV-1 increases the population of aTreg and FOXP3^{low} non-suppressive T cells and induces leukemia/lymphoma of these cells. It is thought that most of nTreg are resting and activated Treg cells and iTreg cells contain both aTreg cells and Foxp3^{low} non-suppressive T cells in human. The CNS2 region in the Foxp3 locus is highly methylated in FOXP3^{low} non-suppressive T cells [44], like we report for the iTreg cells of HBZ-Tg mice. It is likely that a fraction of FOXP3^{low} non-suppressive T cells lose FOXP3 expression and change to FOXP3$^-$ proinflammatory T cells as reported in HAM/TSP patients [40], suggesting that the finding of this study is indeed the case in HTLV-1 infection.

It has been widely believed that nTreg cells represent a highly stable lineage in which few cells lose Foxp3 expression under normal homeostatic conditions [46]. In contrast, small subsets of CD25$^-$Foxp3$^+$ Treg cells have recently been reported to be unstable

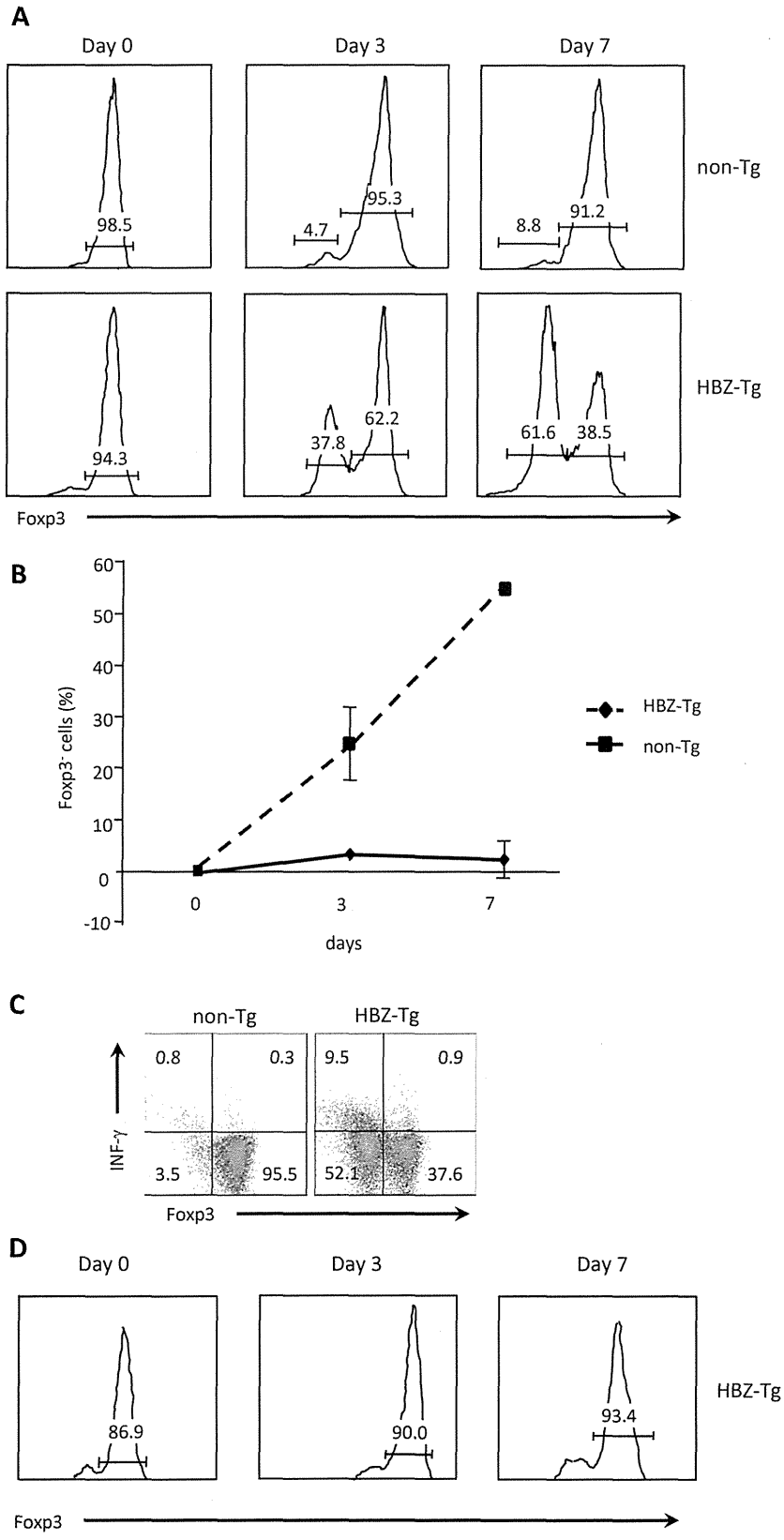

Figure 7. Stability of Foxp3 expression during *ex vivo* culture. (A) Treg cells, sorted from HBZ-Tg or non-Tg mice, were cultured in the presence of IL-2 for 3 or 7 days. The expression of Foxp3 was analyzed by flow cytometry. (B) Sequential changes of the Foxp3$^-$ population are shown. (C) IFN-γ production of *ex vivo* cultured Foxp3$^+$ cells was evaluated by intracellular staining. Sorted Treg cells were cultured for 7 days, and then stimulated for 4 h with PMA/ionomycin and protein transport inhibitor. (D) Foxp3 expression of sorted CD4$^+$CD25$^+$GITR^{high}thymocytes from HBZ-Tg mice.
doi:10.1371/journal.ppat.1003630.g007

and to rapidly lose Foxp3 expression after transfer into a lymphopenic host [16]. The CNS2 sequence is methylated in iTreg cells [24]. Consistent with this finding, CNS2 was heavily methylated in Treg cells of HBZ-Tg mice, indicating that Treg cells in HBZ-Tg mice largely belong to the iTreg cell subset. Foxp3 expression of $CD4^+$ thymocytes in HBZ-Tg mice did not decrease after *in vitro* culture, a fact which shows that loss of Foxp3 expression is not a direct effect of HBZ, but is due to the increased number of iTreg cells converting to exFoxp3 cells. Recently, it was reported that $Foxp3^+$ T cells without suppressive function convert to exFoxp3 T cells [17]. We recently reported that HBZ enhances *Foxp3* gene transcription by activating the TGF-ß/Smad pathway [13]. Collectively, it is likely that HBZ increases $Foxp3^+$ T cells in HBZ-Tg mice and most of $Foxp3^+$ T cells are iTreg and/or non-suppressive $Foxp3^+$ T cells. Foxp3 expression in HBZ-Tg mice is unstable as shown in this study, and such cells easily convert to exFoxp3 T cells, which produce excess amounts of IFN-γ, leading to inflammation.

Helios expression has been reported to be high in nTreg cells, and low in iTreg cells [20]. This study showed that Helios expression in $CD4^+Foxp3^+$ cells of HBZ-Tg mice was low although it was higher than control iTreg cells. Recently, it has been reported that stimulation enhances Helios expression of iTreg cells, which might account for increased Helios expression in $CD4^+Foxp3^+$ cells of HBZ-Tg mice compared with control iTreg cells [22]. In particular, inflammation caused by HBZ expression might increase Helios expression of iTreg cells of HBZ-Tg mice. In addition, it has been reported that Helios is not expressed in a part of nTreg cells and its expression is induced in iTreg cells, indicating that only Helios expression cannot discriminate nTreg cells from iTreg cells [21–23]. However, CNS2 is not methylated in $Helios^-$ nTreg cells, which shows that the methylation status of CNS2 is critical [21]. In this study, analysis of DNA methylation of CNS2 confirms that most of $CD4^+Foxp3^+$ cells in HBZ-Tg mice are iTreg cells. Importantly, the similar pattern of Heilos expression was observed in HAM/TSP patients.

The present study has demonstrated that HBZ-Tg mice develop inflammation in the intestines, skin and lungs. These tissues are always exposed to extrinsic antigens and commensal microbes, where Treg cells are critical for maintaining the homeostasis of the host immune system. In addition to the increased production of IFN-γ by HBZ-expressing cells, it is likely that the cell adhesion attributes of these cells also play a role in their pro-inflammatory phenotype. Treg cells express a variety of molecules that are important for cell adhesion, including LFA-1, CCR4, and CD103 [12]. We have shown that these molecules are also present on HBZ-expressing $CD4^+$ T cells. In this study, we showed that HBZ increases the number of iTreg cells, which subsequently convert into exFoxp3 T cells. The proinflammatory phenotype of HBZ-expressing T cells indicates that HBZ plays an important role in the inflammatory diseases caused by HTLV-1.

In conclusion, HBZ-Tg mice developed chronic inflammation accompanied with hyper IFN-γ production, which is consistent with the findings in HAM/TSP patients. $CD4^+Foxp3^+$ T cells, especially iTreg cells, were increased in HBZ-Tg mice. The expression of Foxp3 was not stable and tended to be lost, which resulted in the enhanced generation of exFoxp3 cells producing IFN-γ. This could be a mechanism for the development of chronic inflammation in HBZ-Tg mice and HTLV-1-infected individuals.

Materials and Methods

Mice and subjects

Transgenic mice expressing HBZ under the murine CD4 promoter have been previously described [12]. Genotypes were determined by means of PCR on mouse ear genomic DNA. All the mice were used at 10–20 weeks of age. Animal experimentation was performed in strict accordance with the Japanese animal welfare bodies (Law No. 105 dated 19 October 1973 modified on 2 June 2006), and the Regulation on Animal Experimentation at Kyoto University. The protocol was approved by the Institutional Animal Research Committee of Kyoto University (permit number: D13-02). All efforts were made to minimize suffering. A total of 10 HAM/TSP patients and 10 healthy donors participated in this study. Written informed consents were obtained from all the subjects in accordance with the Declaration of Helsinki as part of a clinical protocol reviewed and approved by the Institutional Ethics Committee of Kyoto University (approval number: 844). Blood samples were collected from the subjects and peripheral blood mononuclear cells (PBMC) were isolated by Ficoll-Paque Plus (GE Healthcare Bio-Sciences) density gradient centrifugation.

Adhesion of CD4+ T cells to immobilized ICAM-1

Production of recombinant mouse ICAM-1 was performed as described previously [47]. A 96-well plate was coated with 100 µl/well of 0.25 µg/ml mouse mICAM-1-Ig (R&D Systems) at 4°C overnight, followed by blocking with 1% BSA for 30 min. Mouse $CD4^+$ cells were labeled with 2′, 7′-bis-(2-carboxyethyl)-5-(and-6) carboxyfluorescein (Molecular Probes, Inc.), suspended in RPMI 1640 containing 10 mM HEPES (pH 7.4) and 10% FBS, transferred into the coated wells at 5×10^4 cells/well and then incubated at 37°C for 30 min. Non-adherent cells were removed by aspiration. Input and bound cells were quantitated in the 96-well plate using a fluorescence concentration analyzer (IDEXX Corp.).

Cell migration assay

Random cell migration was recorded at 37°C with a culture dish system for live-cell microscopy (DT culture dish system; Bioptechs). Thermoglass-based dishes (Bioptechs) were coated with 0.1 µg/ml mouse ICAM-1. $CD4^+$ mouse splenocytes were loaded in the ICAM-1-coated dish, and the dish was mounted on an inverted confocal laser microscope (model LSM510, Carl Zeiss MicroImaging, Inc.) Phase-contrast images were taken every 15 s for 10 min. The cells were traced and velocity was calculated using ImagePro^R Plus software (Media Cybernetics).

Flow cytometric analyses

Single-cell suspensions of mouse spleen, lung or PBMC or human PBMC were made in RPMI 1640 medium supplemented with 10% FBS. To detect Tax, $CD8^+$ cells were depleted from human PBMC using the BD IMAG cell separation system with the anti-human CD8 Particles-DM (BD Pharmingen) according to the manufacturer's directions and then the cells were cultured for 6 hours. Surface antigen expression was analyzed by staining with the following antibodies: anti-mouse CD4 (RM4-5), CD11a (2D7), CD18 (C71/16) or CD103 (M290) (all purchased from BD Pharmingen) or anti-human CD4 (RPA-T4), CD11a (HI111), CXCR3 (G025H7) (all purchased from BioLegend), CD18 (6.7), CD103 (Ber-ACT8) (all purchased from BD Pharmingen). For intracellular cytokine staining, cells were pre-stimulated with 20 ng/ml phorbolmyristate acetate (PMA, NacalaiTesque), 1 µM ionomycin (NacalaiTesque) and Golgi plug (BD Pharmingen) for 4 h prior to surface antigen staining. After this stimulation period, cells were fixed and permeabilized with Fixation/Permeabilization working solution (eBioscience) for 30 min on ice and incubated with antibodies specific for the following cytokines: IFN-γ (XMG 1.2), IL-17 (TC11-18H10), IL-2 (JES6-5H4) (all BD Pharmingen), TNF-α (MP6-XT22, eBioscience) and IL-4 (11B11, eBioscience).

Intracellular expression of mouse Foxp3 (FJK-16s, eBioscience), human FoxP3 (PCH101, eBioscience), Tax (MI73), human IFN-γ (4SB3, BD Pharmingen) and Helios (22F6, BioLegend) was detected following the protocol for cytokine staining. Dead cells were detected by pre-staining the cells with the Live/dead fixable dead cell staining kit (Invitrogen). Subsequently, the cells were washed twice, and analyzed by FACS CantoII with Diva software (BD Biosciences).

Histological analysis

Mouse tissue samples were either fixed in 10% formalin in phosphate buffer and then embedded in paraffin or frozen in embedding medium Optimal Tissue-TeK (SAKURA Finetek Japan). Hematoxylin and eosin staining was performed according to standard procedures. Tissue sections prepared from the frozen samples were also stained with anti-mouse IFN-γ (RMMG-1, Abcam), CD11a (M17/4, BioLegend), CD18 (N18/2, BioLegend), CD103 (M290, BD Pharmingen) and CD54 (ICAM-1)(YN1/1.7.4, BioLegend). Images were captured using a Provis AX80 microscope (Olympus) equipped with an OLYMPUS DP70 digital camera, and detected using a DP manager system (Olympus).

ELISA assay for chemokines

The α chemokines CXCL9 and CXCL10 were analyzed using an enzyme linked immunosorbent assay (ELISA). For α chemokines, capture and detection antibody concentrations were optimized using recombinant chemokines from R&D Systems Inc. (Minneapolis, MN, U.S.A.) according to the manufacturer's guidelines.

Direct sequencing after sodium bisulfite treatment

Genomic DNA was extracted from sorted Treg cells as described below. One mg of genomic DNA (10 μl) was denatured by the addition of an equal volume of 0.6 N NaOH for 15 min, and then 208 μl of 3.6 M sodium bisulfite and 12 μl of 1 mM hydroxyquinone were added. This mixture was incubated at 55°C for 16 hours to convert cytosine to uracil. Treated genomic DNA was subsequently purified using the Wizard clean-up system (Promega), precipitated with ethanol, and resuspended in 100 μml of dH_2O. Sodium bisulfite-treated genomic DNAs (50 ng) were amplified with primers targeting the specified DNA regions, and then PCR products were subcloned into the pGEM-T Easy vector (Promega) for sequencing. Sequences of 10 clones were determined for each region using Big Dye Terminator (Perkin Elmer Applied Biosystems) with an ABI 3100 autosequencer. The primers used for nested PCR were as follows:

for the mouse *Foxp3* promoter:
mproF, 5′-GTGAGGGGAAGAAATTATATTTTTAGATG-3′;
mproR, 5′-ATACTAATAAACTCCTAACACCCACC-3′;
mproF2, 5′-TATATTTTTAGATGATTTGTAAAGGGTAAA-3′;
mproR2, 5′-ATCAACCTAACTTATAAAAAACTACCACAT-3′.
For mouse *Foxp3* intronic CpG:
mintF, 5′-TATTTTTTTGGGTTTTGGGATATTA-3′;
mintR, 5′-AACCAACCAACTTCCTACACTATCTAT-3′;
mintF2, 5′-TTTTGGGTTTTTTTGGTATTTAAGA-3′;
mintR2, 5′-TTAACCAAATTTTTCTACCATTAAC-3′.

Sorting of Treg cells

To sort Treg cells, we isolated mouse splenocytes and resuspended them in FACS buffer for subsequent staining with the following antibodies purchased from BD Pharmingen: anti-mouse CD4 (RM4-5), GITR (DTA-1), CD25 (PC61). $CD4^+CD25^+GITR^{high}$ cells and $CD4^+CD25^-GITR^{low}$cells were sorted as $Foxp3^+$ or $Foxp3^-$cells using FACS AriaII with Diva software (BD Biosciences). To confirm the purity of the sorted Treg cells, we measured the percentage of Foxp3 expression by intracellular staining, as described above. Sorted Treg cells were cultured in RPMI1640 containing 10% FBS, antibiotics, and 50 μM 2-mercaptoethanol (Invitrogen).

Synthesis of cDNA and quantitative RT-PCR

Total RNA of sorted cells was extracted with TRIZOL reagent (Invitrogen) according to the manufacturer's instructions. Approximately 200 ng of RNA were used to prepare cDNA using the SuperScript III enzyme (Invitrogen). Levels of *HBZ* and *Foxp3* transcripts were determined with FastStart Universal SYBR Green Master reagent (Roche) in a StepOnePlus real time PCR system (Apllied Biosystems). Data was analyzed by the delta Ct method. The sequence of the primers used were as follows:

HBZ Forward: 5′-GGACGCAGTTCAGGAGGCAC-3′, Reverse: 5′-CCTCCAAGGATAATAGCCCG-3′; *Foxp3* Forward: 5′-CCCATCCCCAGGAGTCTTG-3′, Reverse: 5′-ACCATGACTAGGGGCACTGTA-3′; 18S rRNA Forward: 5′-GTAACCCGTTGAACCCCATT-3′, Reverse: 5′- CCATCCAATCGGTAGTAGCG -3′.

Supporting Information

Figure S1 Expression of CCR5 and CCR7 on $CD4^+$ T cells and production of CXCL9 and CXCL10 in HBZ-Tg mice. Expression of CCR5 (A) and CCR7 (B) on $CD4^+$ T cells was analyzed by flow cytometry. (C) CXCL9 (left) and CXCL10 (right) in sera of HBZ-Tg or non-Tg mice were measured by ELISA. The data shown mean ± SD of triplicates.
(PPTX)

Figure S2 Expression of Helios in $CD4^+Foxp3^+$ T cells in spleen and lung. Expression of Heilos of $Foxp3^+CD4^+$ T cells was analyzed in lungs (upper panels) and spleen (lower panels) from HBZ-Tg mice and non-Tg mice.
(PPTX)

Figure S3 Helios expression in thymocytes. Expression of Helios in $CD4^+$ $Foxp3^+$ cells of HBZ-Tg mouse (solid line) is compared to that of non-Tg mouse (dashed line) and isotype control (filled histogram). One representative result of three independent experiments is shown.
(PPTX)

Figure S4 HBZ expression is not correlated with Foxp3 expression in HBZ-Tg mice. (A) The proportion of $Foxp3^+$ cells in the Foxp3 (+) and Foxp3 (−) sorted populations was of 91.2% and 42.6%, respectively, when determined by intracellular staining. Expression of *HBZ* (B) and *Foxp3* (C) as measured by qRT-PCR in the sorted populations as described in material and methods. The expression level in whole CD4 cells from HBZ or WT mice were used as reference for *HBZ* and *Foxp3*, respectively.
(PPTX)

Acknowledgments

We thank Linda Kingsbury for kind revision of the manuscript.

Author Contributions

Conceived and designed the experiments: NYT YS MM. Performed the experiments: NYT YS PM KO KK. Analyzed the data: NYT YS TK MM. Contributed reagents/materials/analysis tools: MN. Wrote the paper: NYT YS PM KK TK MM.